Available online at www.sciencedirect.com
SCIENCE DIRECT®
Applied Geochemistry 20 (2005) 767–787
Applied Geochemistry
www.elsevier.com/locate/apgeochem

Groundwater in the Broken Hill region, Australia: recognising interaction with bedrock and mineralisation using S, Sr and Pb isotopes

Patrice de Caritat [a,*], Dirk Kirste [a,1], Graham Carr [b], Malcolm McCulloch [c]

[a] *Cooperative Research Centre for Landscape Environments and Mineral Exploration, c/- Geoscience Australia, GPO Box 378, Canberra, ACT 2601, Australia*
[b] *CSIRO Division of Exploration and Mining, PO Box 136, North Ryde, NSW 1670, Australia*
[c] *Research School of Earth Sciences, The Australian National University, Canberra, ACT 0200, Australia*

Abstract

The supergiant Pb–Zn–Ag Broken Hill orebody and numerous other minor mineral deposits occur within the limited outcrop of the Proterozoic Curnamona Province of Australia. The vast majority of this Province is concealed by up to 200 m of transported regolith, hampering conventional exploration strategies. Approximately 300 groundwater samples were collected over the southern Curnamona Province to test whether this medium could be helpful in the search for hidden mineral deposits. Sulphur, Sr and Pb isotope composition of the groundwaters were determined and S excess (S_{XS}), i.e., the amount of S that can be ascribed neither to evaporation nor to mixing, was calculated. Many samples were recognised to have undergone an addition of ^{34}S-depleted S, which can be attributed to oxidation of sulfides with a Broken Hill type δ^{34}S signature (average ~0‰ V-CDT). Furthermore, Sr isotopes identify the broad types of bedrock that the groundwater has been interacting with, from the less radiogenic Adelaidean rocks (and minerals) in the west (groundwater ^{87}Sr/^{86}Sr ratio as low as 0.708) to the highly radiogenic Willyama Supergroup in the east (^{87}Sr/^{86}Sr ratio up to 0.737). The groundwaters have ^{207}Pb/^{204}Pb and ^{206}Pb/^{204}Pb ratios comparable to, or intermediate between, various mineralisation types recognised in the area (Broken Hill, Rupee, Thackaringa, etc., types). The few samples taken in the vicinity of known mineralisation yield positive indicators (positive S_{XS}, low δ^{34}S, ^{87}Sr/^{86}Sr signature of bedrock type and Pb isotope fingerprinting of mineralisation type). This study also highlights several new locations under sedimentary cover where these indicators suggest interaction with mineralisation.

1. Introduction

As a result of the increasing exploration maturity of many mineral provinces worldwide, the search for ore deposits is increasingly focusing onto areas where the potentially mineralized bedrock is not visible at the Earth's surface. Here, potentially thick in situ or transported regolith material obscures the geochemical and geophysical responses from underlying orebodies and

* Corresponding author. Fax: +61 2 6249 9930.
E-mail address: patrice.decaritat@ga.gov.au (P. de Caritat).
[1] Present address: Cooperative Research Centre for Landscape Environments and Mineral Exploration, c/- Department of Earth and Marine Sciences, The Australian National University, Canberra, ACT 0200, Australia.

0883-2927/$ - see front matter
doi:10.1016/j.apgeochem.2004.11.003

alteration products. This is especially of concern where the regolith cover is greater than a few meters thick, and, especially, where it is allochthonous or transported. These situations are common in many countries around the world, including Australia, Canada, Chile, USA, etc., which attract a significant part of the world's exploration investments. In order to be successful in these terrains, exploration strategies different from those used in areas of bedrock outcrop or subcrop must be called upon, and special exploration tools are needed to deal with these virtually unexplored frontiers. Hydrogeochemistry is one such tool, and in this contribution the authors investigate the potential for using S, Sr and Pb isotopes coupled to standard water chemistry to recognize groundwater-basement interaction and to vector toward mineralisation under cover.

Groundwater geochemistry has been used in mineral exploration for a number of years. It was particularly popular in the 1970s (Taufen, 1997), when it was commonly applied to U exploration (Clarke and Kugler, 1973; Earle and Drever, 1982; Dean et al., 1982; Miller et al., 1984). Hydrogeochemical exploration has experienced renewed interest in the last few years (Giblin and Mazzucchelli, 1997; Leybourne et al., 1998; Pauwels et al., 1999, 2002; Caritat et al., 2001; Sader et al., 2003), and is likely to become more and more popular as technological developments and increasing affordability continue, and the drive to exploration under cover persists. The combined use of isotopes and trace elements in groundwaters in Australian conditions has previously been reported by Andrew et al. (1998), Whitford et al. (1998) and Caritat et al. (2001).

The advantages of hydrogeochemistry in exploration through thick regolith are that:

(1) groundwater is a medium that has the potential to have been in direct contact with mineralisation;
(2) groundwater is relatively easily and cheaply retrieved and analysed with high-performance equipment;
(3) mineralisation may be located either in the basement rocks (e.g., fractures, alteration zones around VMS or vein-type deposits) or within the cover sequence (e.g., MVT deposits, U roll-front deposits);
(4) exploration is not model-driven (sampling points are, in the most part, where pastoralists have drilled water bores, not where geophysics reveals 'blobs'); and
(5) exploration is not commodity specific (multi-element analysis may reveal unexpected element accumulations).

If the groundwater has interacted with mineralisation at depth, it will have changed major, minor, trace element and/or isotope character. If such a geochemical signature is preserved and transported long enough to reach a bore from which groundwater can be sampled, then there is potential for this medium to be very useful in mineral exploration. A hydrogeochemical exploration survey based on previously existing sampling points (bores, wells, springs, seepages) is likely to be of regional usefulness only at first, unless the density of such points is relatively high. Once a sub-area has been identified by hydrogeochemistry as having a high potential to host a blind ore deposit, more detailed (and expensive) exploration tools, such as drilling, can be focused on this much smaller area, thus enabling potentially huge cost savings.

The area for the present study is the Broken Hill region, which is host to a single known supergiant Pb–Zn–Ag orebody (~300 Mt; Stevens and Burton, 1998) and numerous smaller Pb–Zn–Ag, Cu–Au, Sn, W and U deposits. These occur mainly in the Paleo- to Neoproterozoic basement rock sequences, which crop out in the Barrier, Olary and Flinders Ranges. Those areas of exposed basement have undergone mineral exploration for more than 100 a, yet additional significant mineral discoveries have been limited.

The Barrier, Olary and Flinders Ranges form the arcuate eastern, southern and western margins, respectively, of the Callabonna Sub-basin (Fig. 1). The latter is a southern depocenter of the larger Lake Eyre Basin of central Australia. The Tertiary sediments and Quaternary soils in the southern Callabonna Sub-basin are up to 200 m thick and conceal ~90% of the highly prospective Proterozoic basement of the Curnamona Province. In the northern part of the Sub-basin, Mesozoic strata from the Great Australian Basin form a southerly thinning wedge of intervening transported material between the basement and the Cenozoic units.

2. Geological setting

The Curnamona Province consists of a sequence of Broken Hill equivalent rocks and Adelaidean rocks (Fig. 1). The former include complexly deformed high-grade metamorphic rocks of the Early Proterozoic Willyama Supergroup; the latter are more gently folded, mostly lower greenschist-grade Late Proterozoic sediments with minor volcanic rocks. This basement is covered by Mesozoic (only along the northern edge of the study area and beyond) and Cenozoic sediments. Detailed accounts of the geology of the Broken Hill Domain (see Fig. 1) have been reported in a number of studies (e.g., Stevens, 1980, 1986; Willis et al., 1983; Page and Laing, 1992; Stevens and Corbett, 1993).

The Willyama Supergroup comprises aluminous metasedimentary gneisses, plus locally abundant albite-rich rocks, basic gneisses (amphibolites), lesser quartzo-feldspathic gneisses and substantial bodies of deformed pegmatite and leucocratic quartzo-feldspathic rocks. The Willyama Supergroup can be found within the

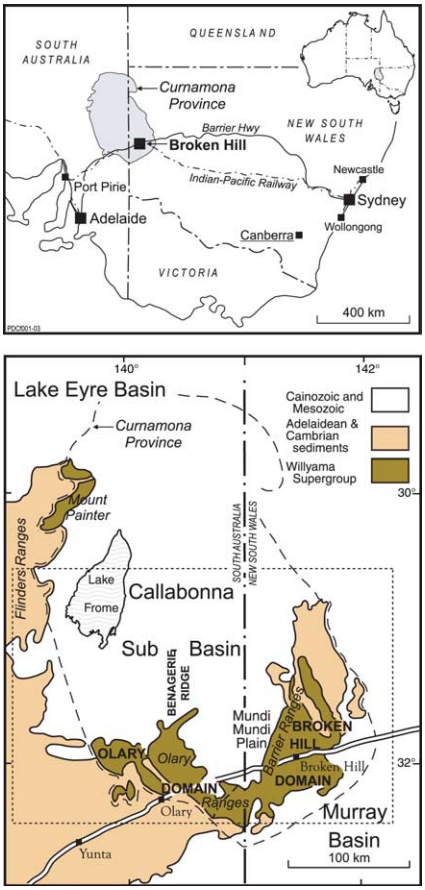

Fig. 1. Location of the study area (dashed rectangle) in the southern Curnamona province.

Broken Hill Domain, where it includes the Thackaringa and Broken Hill Groups, the Olary Domain, and the Redan Geophysical Zone, which both contain abundant albitite and calc-albitite (Stevens and Corbett, 1993). The Adelaidean sequence unconformably overlies the Willyama Supergroup and can be correlated with the more extensive occurrence of Adelaidean rocks in South Australia (Cooper et al., 1978; Preiss, 2000). It consists of a sequence of quartzite, quartzite conglomerate, limestone, siltstone, sandstone, shale, dolomite and diamictite forming various groups (Willis et al., 1983; Stevens et al., 1988; Stevens and Corbett, 1993). In the southern Curnamona Province, downthrown Proterozoic rocks west of the Broken Hill Domain are overlain by a thick fluvio-lacustrine sedimentary succession belonging to the Cenozoic Lake Eyre Basin, which extends across a vast area of central Australia. This basin is interpreted to have formed by tectonic subsidence in northeastern South Australia during the Late Paleocene (Callen et al., 1995). The Lake Eyre Basin comprises a number of sub-basins, including the Callabonna Sub-basin that covers most of the study area. Quaternary sediments and soils commonly cover Tertiary units. Deposition in the Lake Eyre Basin occurred in 3 phases, described below (Callen et al., 1995).

(1) In the first phase, sandstone, carbonaceous clastics and conglomerate of the Eyre Formation were deposited during the latest Paleocene to Middle Eocene.
(2) The second phase includes deposition of grey, green and white clay, fine-grained sand and carbonate, with minor conglomerate of the Namba Formation during the Oligocene to Pliocene. It is informally divided into a lower member characterized by smectite and cyclic deposition, and an upper member with illite and kaolinite. The Namba Formation was deposited in low-energy lacustrine environments (Callen, 1990).
(3) The third phase was characterized by the deposition of red and yellow-brown sand and sandy clay, and the development of gypsum and carbonate paleosols during the Pliocene to Quaternary.

The regional regolith and landscape features of the Broken Hill region are now being extensively studied. Recent works include those of Hill et al. (2000), Hill (2000), Gibson (2000) and Caritat et al. (2000a,b, 2001). Depth to fresh bedrock in the region varies from minimal in bedrock-dominated terrains up to approximately 200 m under basin cover (Caritat et al., 2000a). The dominant regolith materials in the region include saprolite, sediments, soils, ferricretes, silcretes, siliceous and/or ferruginous lags and carbonate accumulations (e.g., Hill, 2000; Hill et al., 2000). Areas of deepest weathering occur in areas of high preservation potential, including down-tilted fault block margins, under duricrust or lag-strewn surfaces, and in localised areas isolated from regional erosion or base-level lowering (Hill, 2000). Tonui et al. (2003) demonstrated that regolith geochemistry is a potentially useful tool for mineral exploration under cover in the Curnamona Province.

3. Methods

3.1. Field

Approximately 280 groundwater samples (omitting duplicates) have been collected from the Broken Hill region (Fig. 2), both from areas of outcrop in the ranges and from the vast expanses of sedimentary cover in the surrounding basins (Caritat et al., 2001, 2002; Kirste and Caritat, 2002). These samples have been analysed for a comprehensive suite of major, minor and trace elements as well as for several stable and radiogenic

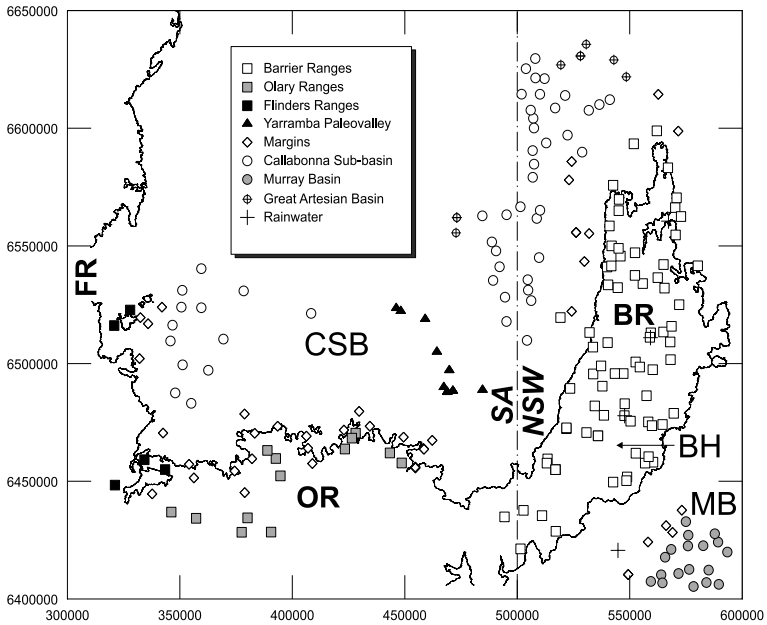

Fig. 2. Sample locations and symbols key. Locations are: BH, Broken Hill; FR, Flinders Ranges; OR, Olary Ranges; BR, Barrier Ranges; CSB, Callabonna Sub-basin; MB, Murray Basin; SA/NSW, South Australia-New South Wales state border. Coordinates: meters UTM Zone 54 WGS84; Outline: 200 m elevation contour.

isotopes. Here, this paper will focus on a subset of 164 samples for which S, Sr and/or Pb isotope data have been obtained.

The groundwater samples were collected mostly from existing stock water bores, the remainder being from exploration drillholes. Many water bores in the region were equipped with functioning pumps driven by windmills, submersible or helical pumps. Open holes were pumped with a Bennett® sampling pump. Every effort was made to obtain uncontaminated groundwater samples representative of aquifer conditions suitable for isotopic and trace element analysis.

3.2. Sulfur isotopes and sulfate concentrations

The S isotopic composition of SO_4^{2-} dissolved in groundwater was obtained from 159 samples. Depending on conductivity, a 250 or a 500 mL sample of freshly pumped and filtered groundwater was collected in a new high-density polyethylene (HDPE) sampling bottle. Filtration in the field was carried out using a 90 mm diameter Pall Gelman Supor® 0.45 μm hydrophillic polyethersulfone membrane filter held in a cleaned custom-built plexiglass vacuum filtering unit. The collected sample was then acidified at a rate of ~1 mL of ultrapure HNO_3 per 1000 mL of sample to prevent carbonate precipitation. Excess $BaCl_2$ was added to form a stable $BaSO_4$ precipitate, which was subsequently separated by filtration in the laboratory, rinsed and dried. The $BaSO_4$ precipitate was sent to the Isotope Science Laboratory, Department of Physics and Astronomy, University of Calgary (Canada), for S isotope analysis on a Carlo Erba® NA 1500 elemental analyzer interfaced with a VG® Prism II mass spectrometer. High temperature reaction of the $BaSO_4$ with V_2O_5 and SiO_2 generated SO_2 for $\delta^{34}S$ measurements (Yanagisawa and Sakai, 1983; Ueda and Krouse, 1986). Sulphur isotope compositions are reported using the conventional $\delta^{34}S$ scale in parts per thousand, ‰:

$$\delta^{34}S_{\text{sample}}(‰) = \frac{R_{\text{sample}} - R_{\text{standard}}}{R_{\text{standard}}} \cdot 1000, \quad (1)$$

where R is the $^{34}S/^{32}S$ abundance ratio of a sample or a standard, as indicated by the subscript. The standard for $\delta^{34}S$ measurements is the V-CDT standard, as established by the International Atomic Energy Agency (IAEA), Vienna. Eight analyses of NBS127 ($BaSO_4$) standard reference material ($\delta^{34}S = +20.32 \pm 0.36$‰) gave a mean $\delta^{34}S$ isotopic composition of $+20.0715 \pm 0.5139$‰ (1σ), resulting in an accuracy bias of ±1.22%. The relative standard deviation (RSD) of 16 samples run at least in triplicate ranged from 0.47% to 6.45% and averaged 2.91% (precision). The RSD on 11 field duplicates ranged from 0.06% to 6.97% and averaged 2.29% (repeatability of sampling).

Dissolved SO_4^{2-} concentrations were measured by ion chromatography on a Dionex® 4000i IC at the Bureau of Rural Sciences, Canberra. Samples consisted of

unacidified, field-filtered aliquots diluted to allow bracketing by prepared standards. All samples were run in duplicate with accuracy and precision within 3%. (Measurements of Cl^- and Br^-, mentioned below, were performed the same way.)

3.3. Strontium isotopes and concentrations

The Sr isotopic composition of dissolved Sr was obtained from 38 groundwater samples representing a wide range of locations and groundwater compositions. A 125 mL sample of freshly pumped, filtered and acidified groundwater (as per above) was collected in a new HDPE Nalgene® sampling bottle rinsed 3 times with filtered sample water (this sample was used for major cation, trace cation and Sr isotope analysis; no contamination was detected). Upon return from the field, a 10 mL aliquot of each selected sample was separated for Sr isotope analysis, which was carried out on a Thermo-Finnigan-MAT® Neptune multi-collector inductively coupled mass spectrometer (MC-ICP-MS) at the Research School of Earth Sciences, The Australian National University, Canberra. Eleven aliquots were analysed there also on a more conventional Thermo-Finnigan-MAT® Triton thermal ionisation mass spectrometer (TIMS) as well as on the MC-ICP-MS. Results are reported as $^{87}Sr/^{86}Sr$ ratios relative to a value of 0.710250 for standard reference material NBS987 ($SrCO_3$). Strontium isotope analyses were performed with a precision of ±0.000010 and an accuracy of ±0.000020 (based on repeat analyses of NBS987). The MC-ICP-MS and TIMS results are in excellent agreement (Table 1).

Dissolved Sr concentrations were measured by ICP-MS at the Ecochemistry Laboratory, University of Canberra, on a different aliquot of the same acidified, field-filtered sample. (Measurement of Zn, mentioned below, was performed the same way.)

3.4. Lead isotopes and concentrations

The Pb isotopic composition of dissolved Pb was obtained from 29 samples selected mainly on the basis of their anomalous S concentration (see below) and low $\delta^{34}S$ composition. A 1000 mL sample of freshly pumped, filtered and acidified groundwater (as per for Sr above) was collected in a new, rinsed HDPE sampling bottle. Contamination was deemed minimal based on the lack of correlation between Pb concentrations (by TIMS) and the $^{206}Pb/^{204}Pb$ data, and the significantly different Pb isotope signatures of the PVC casing and the groundwater sample as tested at one location.

The Pb was initially concentrated on a Chelex® ion exchange resin (at pH 5) then separated by anion exchange chromatography. The Pb was loaded onto single Re filaments and isotope ratios were determined on a VG® ISOMASS 54E solid source TIMS at the CSIRO Division of Exploration and Mining, Sydney, with a typical precision of ±0.05% (2σ) for the $^{207}Pb/^{204}Pb$ ratio. Data have been normalised to the accepted values of international standard NBS981 by applying a correction factor of +0.08% per atomic mass unit. Results are reported as $^{206}Pb/^{204}Pb$, $^{207}Pb/^{204}Pb$ and $^{208}Pb/^{204}Pb$ ratios.

Dissolved Pb concentrations were measured by ICP-MS at the Ecochemistry Laboratory, University of Canberra, on acidified, field-filtered samples, as per the Sr discussed above. The dissolved Pb was determined again as part of the sample preparation for the isotope analysis after being concentrated by ion exchange, then measured by TIMS at the CSIRO Division of Exploration and Mining, Sydney.

3.5. Quality assurance and quality control (QA/QC)

All efforts were made throughout the project to ensure internal consistency and avoid contamination from sampling to analysis. This was achieved by using clean sampling equipment from the same source and following clear sampling protocols. Avoidance of contamination was best achieved by purging the bores before sampling, using new, quality sampling containers triply rinsed (with the water to be sampled), wearing powder-free latex gloves and not allowing smoking during sample manipulation. Preparation and analysis of all the samples were performed in the same laboratories. Additional QA procedures included: (1) analysis of rinse and travel blanks; (2) analysis of a number of control reference materials; (3) analysis in duplicate of 1 in every 10 samples; (4) analysis of field duplicate samples; and (5) verification of charge balances.

4. Results and discussion

The isotopic compositions of the groundwater samples, as well as a statistical summary, are given in Table 1. The $\delta^{34}S$ values range from +2.29‰ to +23.53‰ (V-CDT), with a median value of +12.71‰. The $^{87}Sr/^{86}Sr$ ratios range from 0.70797 to 0.73709, with a median value of 0.71949. The $^{206}Pb/^{204}Pb$ ratios range from 16.213 to 18.576, with a median value of 17.212. The $^{207}Pb/^{204}Pb$ ratios range from 15.406 to 15.840, with a median value of 15.538. The $^{208}Pb/^{204}Pb$ ratios range from 35.898 to 38.397, with a median value of 36.927. Fig. 3 shows the regional distributions of the S, Sr and Pb isotopic results, based on boxplot-derived classes.

4.1. Sulfur system

Sulfate dissolved in groundwater from the Curnamona Province is weakly correlated to Cl^-, with

Table 1
Location details, concentrations of dissolved Cl^-, SO_4^{2-}, Sr, Pb and Zn, and isotope compositions $\delta^{34}S(SO_4^{2-})$, $^{87}Sr/^{86}Sr$ (two methods), $^{206}Pb/^{204}Pb$, $^{207}Pb/^{204}Pb$ and $^{208}Pb/^{204}Pb$ of the groundwater samples from the Curnamona Province region

ID	Site	Date	Eastings (m)	Northings (m)	Cl^- (mg/L)	SO_4^{2-} (mg/L)	Sr (mg/L)	Pb (mg/L)	Zn (mg/L)	$\delta^{34}S$ (‰ V-CDT)	$^{87}Sr/^{86}Sr$ [a]	$^{87}Sr/^{86}Sr$ [b]	$^{206}Pb/^{204}Pb$	$^{207}Pb/^{204}Pb$	$^{208}Pb/^{204}Pb$
BH001	Zacks Bore	9/9/99	464264	6505035	4500	1340	9.09	<0.001	0.4658	12.45	0.72114	0.72115			
BH002	Pasminco Jacks Dam	9/9/99	459041	6518933	12800	2350	17.64	<0.001	0.0027	12.28	0.71784				
BH004	Pasminco Benagerie Bore	9/9/99	446170	6523590	8760	2040	10.83	<0.001	<0.001	13.87					
BH005	Big Nancatee Bore	9/11/99	429700	6479700	1900	1790	8.19	<0.001	0.0775	13.01	0.71520	0.71518			
BH006	Pasminco Turkeys Nest	9/11/99	448211	6522347	5610	1520	8.02	<0.001	<0.001	13.38	0.72128	0.72129			
BH008	Torrominga bore	9/11/99	428150	6470432	3120	1650	6.91	<0.001	<0.001	9.73					
BH009	Jasons Bore	9/12/99	469789	6497195	4700	1510	8.48	0.0010	0.0317	12.44	0.72267	0.72267			
BH011	Brooks Dam Bore	9/12/99	467341	6490013	4640	1330	8.56	<0.001	<0.001	13.60					
BH012	Cultivation Bore (Pump Jack)	9/13/99	458292	6463925	898	1070	3.49	<0.001	0.5539	13.28					
BH014	Oonatra Dam Bore	9/14/99	448641	6457742	2750	2030	5.43	0.0010	<0.001	5.74			18.115	15.579	37.314
BH015	Bullocks Bush Bore	9/14/99	449445	6468753	2370	995	4.39	<0.001	0.0286	11.69					
BH016	Oonatra Bore 1	9/14/99	454653	6456088	2510	933	3.72	<0.001	<0.001	12.78	0.72223	0.72223			
BH017	Oonatra Bore 2	9/14/99	454707	6455667	2520	1410	5.04	<0.001	0.0022	11.04					
BH018	Black Oaks/Boundary Bore	9/15/99	426482	6468314	2550	870	6.18	<0.001	<0.001	10.62					
BH019	Pootharingla Well	9/15/99	434477	6473402	3460	2220	9.56	<0.001	0.0501	11.84					
BH021	Torrominga bore (south)	9/15/99	423399	6463697	2450	1500	6.01	<0.001	0.0028	11.75					
BH022	Cultivation Bore (Windmill)	9/15/99	458529	6463610	2140	1520	4.33	<0.001	<0.001	12.60					
BH023	Ironstone Bore	9/16/99	422949	6471761	2740	1650	6.64	<0.001	0.0832	10.45					
BH024	Wiparaminga Bore	9/16/99	443395	6462014	996	593	2.03	<0.001	<0.001	10.15	0.72509	0.72511			
BH025	Millierooka Bore	9/17/99	462203	6467384	1810	738	2.90	<0.001	0.0115	11.24					
BH026	Four Corners Bore	9/17/99	484560	6488854	4580	1290	7.60	<0.001	1.4769	13.23	0.72283	0.72282			
BH030	Wallaces Bore	9/18/99	495227	6517886	2280	893	3.71	0.0025	0.0834	13.07			18.576	15.566	38.282
BH031	Lockhart Bore	9/18/99	494555	6528214	2260	786	2.99	<0.001	0.4283	12.27					
BH032	New Chum extension	9/18/99	489274	6535305	2390	799	4.28	<0.001	0.0010	13.86	0.71971				
BH033	Corona Bore	9/19/99	495260	6563235	1450	495	2.67	<0.001	0.0090	15.36					
BH034	Glenroy Bore	9/19/99	484493	6562752	1750	696	2.41	<0.001	0.0244	12.79	0.72091	0.72095			
BH035	Birksgate Bore (Diesel)	9/19/99	473125	6562038	822	0.25	0.73	<0.001	0.0150	6.40					
BH036	Birksgate Bore (Windmill)	9/19/99	473126	6562031	793	0.25	0.72	<0.001	0.0092	11.19					
BH037	Lake Charles Bore	9/19/99	472796	6555549	2930	273	2.13	<0.001	0.0070	16.39	0.71792				
BH038	Furlough Bore	9/20/99	492160	6541129	1620	673	2.58	<0.001	0.1222	13.00					
BH039	Watsons Bore	9/20/99	490569	6547863	1760	728	3.25	<0.001	0.0069	13.52					
BH040	Glenapp Bore	9/20/99	488730	6551663	2240	975	3.87	<0.001	0.0172	13.46					
BH042	WMONB	9/22/99	468848	6487930	5050	1640	8.55	<0.001	<0.001	13.85					
BH043	WMONM	9/22/99	468848	6487914	4580	1410	7.54	<0.001	0.0101	12.17					
BH044	WMONU	9/22/99	468847	6487898	4540	1360	7.24	<0.001	<0.001	13.16					
BH046	EMONB	9/23/99	471384	6488383	5350	1770	8.96	<0.001	0.0066	13.27					
BH047	EMONM	9/23/99	471385	6488366	4710	1530	8.03	<0.001	0.0040	13.21					
BH048	EMONU	9/23/99	471385	6488349	4570	1300	7.51	<0.001	0.0027	13.37					
BH100	Zig Zag Bore	2/3/00	544679	6532250	1360	993	1.10	<0.001	0.0148	16.46					
BH101	Alberta Well	2/3/00	540392	6533442	1260	764	2.66	<0.001	0.0154	14.34					
BH102	Old Corona Well	2/3/00	539951	6541038	1800	829	3.01	0.0018	0.0115	13.22					

BH103	Near Neds Tank	2/3/00	529847	6543369	3510	1810	6.20	<0.001	<0.001	12.88					
BH104	South Bore	2/4/00	504325	6509845	1500	664	2.36	<0.001	<0.001	12.24	0.73167	0.73170			
BH105	Warners Bore	2/4/00	519210	6519534	515	253	0.98	<0.001	<0.001	14.30					
BH106	Stevens Bore	2/4/00	524201	6522198	1110	734	3.29	<0.001	<0.001	12.74					
BH107	Brewery Bore	2/5/00	540202	6508905	3520	2570	6.61	<0.001	0.0216	12.64	0.72225				
BH108	Poolamacca Well	2/5/00	533667	6506993	4520	2330	3.74	0.0019	0.0687	11.38			17.465	15.489	37.116
BH109	Homestead Bore	2/5/00	532144	6513201	1710	881	3.57	<0.001	0.0220	13.20					
BH113	House Bore	2/6/00	526186	6555740	3110	1000	2.78	<0.001	0.0020	13.27					
BH114	McDougalls Well	2/6/00	526124	6555711	786	341	0.86	<0.001	0.0045	13.74	0.72057	0.72055			
BH115	Three Corners	2/6/00	541963	6550007	936	740	2.29	0.0012	0.0082	6.25	0.72114		16.973	15.544	36.786
BH116	Copper Mine Bore	2/6/00	545925	6545652	1160	577	1.03	0.0022	0.0055	13.05					
BH117	Border Bore	2/7/00	501441	6566624	4860	1600	6.60	0.0131	0.0012	15.58			17.183	15.558	36.944
BH118	Glenmore Bore	2/7/00	508692	6561679	3260	1190	5.21	<0.001	<0.001	15.21					
BH119	Mount Bull Bore	2/7/00	510142	6565117	2460	766	3.04	<0.001	0.1557	12.72					
BH120	Nickatime Bore	2/8/00	541041	6558483	1870	2100	5.74	<0.001	0.0557	7.90					
BH121	Corner Bore	2/8/00	545122	6564978	1600	2100	2.96	<0.001	0.0087	8.80					
BH122	Gormans Bore	2/8/00	545250	6569751	1320	1610	4.84	<0.001	0.1404	10.09					
BH123	Texs Bore	2/9/00	509711	6545031	1370	886	3.03	<0.001	0.0609	12.91					
BH125	Kulka Bore	2/9/00	504676	6535630	984	850	2.01	<0.001	0.1584	13.70					
BH126	Danzie Bore	2/9/00	504859	6531184	1300	1410	3.29	<0.001	0.2192	13.05					
BH127	Mulga Valley Bore	2/9/00	506201	6526759	2200	1810	5.24	<0.001	0.1749	12.87					
BH128	Old Corona Well Bore	2/9/00	541834	6541485	394	201	0.70	<0.001	0.0048	11.83					
BH129	Four Corners Bore	2/10/00	531944	6555260	1870	635	1.84	<0.001	0.0020	13.70					
BH130	Eight Mile Bore	2/10/00	545045	6548955	2570	1680	5.64	<0.001	0.0215	11.06					
BH131	Black Tank Bore	2/10/00	552365	6547093	5880	2750	17.58	0.0032	0.0147	12.14					
BH132	Silverton Commons Borehole 1	2/11/00	521851	6472345	3590	2110	2.81	<0.001	0.0207	8.70					
BH151	Mundi Mundi Ck Well	6/1/00	523518	6489444	4210	2400	6.00	0.0011	<0.001	12.09					
BH152	Sundown Borehole	6/2/00	516997	6454920	1410	1270	1.70	0.0024	0.2581	5.49			18.562	15.626	37.753
BH153	Mt George Borehole	6/2/00	513488	6459454	332	654	1.08	<0.001	0.0545	2.29	0.72223	0.72224	18.539	15.615	37.255
BH154	Mt George Well	6/2/00	513144	6457685	3860	2680	5.73	<0.001	0.0045	9.89					
BH155	Penrose Park #1	6/3/00	521866	6472679	12000	4150	22.05	<0.001	0.0021	8.63					
BH158	Limestone Well	6/3/00	530785	6470670	2010	1320	3.52	0.0092	0.0993	7.72			18.432	15.840	38.397
BH159	House Bore	6/3/00	535909	6469290	884	472	1.34	0.0010	<0.001	8.70			17.751	15.754	37.743
BH201	Ninnerie Dam Bore	2/28/01	392686	6459671	368	210	0.85	<0.001	0.0990	12.19					
BH202	Mt Victoria Hut Bore	2/28/01	388924	6463088	1448	516	2.71	<0.001	0.2357	11.30					
BH203	Parkinsons Bore	2/28/01	393488	6473373	1737	724	2.68	<0.001	0.1169	11.50	0.71945				
BH204	North Koolka Bore	2/28/01	406258	6469170	2734	1982	7.37	<0.001	0.2074	9.74			17.626	15.598	36.966
BH205	Weeroopie Well	3/1/01	406967	6464014	1177	1936	2.60	<0.001	0.0447	12.75			17.927	15.781	37.538
BH206	Morts Bore	3/1/01	408910	6457527	3338	1566	6.93	<0.001	1.0199	10.04			16.803	15.478	36.499
BH209	Arkaroola Bore	3/2/01	374346	6454351	1943	914	5.41	<0.001	0.0875	12.70					
BH210	Marshes Bore	3/2/01	382071	6459561	1953	756	5.06	<0.001	0.8802	13.01					
BH212	Jagged Rocks Bore	3/2/01	383272	6470382	695	236	1.37	<0.001	2.8385	12.60			18.247	15.624	37.644
BH213	North Toweroo Bore	3/2/01	378754	6478579	1118	588	2.38	<0.001	0.4485	11.93					
BH214	Gums Well	3/3/01	378826	6445194	5306	1975	16.24	<0.001	0.1038	16.67	0.71520				
BH215	Diggings Bore	3/3/01	377491	6428307	4214	2337	9.07	<0.001	0.0229	22.20	0.71614				
BH216	Pipeline Bore	3/3/01	380100	6434422	749	588	1.32	<0.001	0.0281	14.37					
BH217	Goldmine Bore	3/3/01	390566	6428394	625	283	0.92	<0.001	0.0176	12.03					
BH218	Old Woolshed Bore	3/4/01	351222	6499456	5224	1723	11.40	<0.001	0.0500	14.15	0.71505				
BH220	Round Hill Bore	3/4/01	347948	6487504	2940	599	6.33	<0.001	0.2934	17.01					

(*continued on next page*)

Table 1 (*continued*)

ID	Site	Date	Eastings (m)	Northings (m)	Cl^- (mg/L)	SO_4^{2-} (mg/L)	Sr (mg/L)	Pb (mg/L)	Zn (mg/L)	$\delta^{34}S$ (‰ V-CDT)	$^{87}Sr/^{86}Sr$ [a]	$^{87}Sr/^{86}Sr$ [b]	$^{206}Pb/^{204}Pb$	$^{207}Pb/^{204}Pb$	$^{208}Pb/^{204}Pb$
BH221	Toolaby Bore	3/4/01	355077	6483098	4888	857	8.40	<0.001	0.1042	15.66					
BH223	Traceys Bore	3/5/01	342528	6470489	1114	277	5.23	<0.001	0.0162	19.44					
BH224	Hills Well Bore	3/6/01	343445	6454952	1119	1793	14.02	<0.001	0.5700	14.96	0.71509				
BH225	Parsons Bore	3/6/01	334244	6459134	1526	487	4.83	<0.001	0.2521	15.98					
BH227	Johnsons Bore	3/6/01	321150	6448350	1696	854	7.85	<0.001	0.2182	12.66	0.71502				
BH228	Oopina Bore	3/7/01	357225	6434243	4025	1615	6.22	<0.001	0.0189	9.95					
BH229	Comet Bore	3/7/01	346222	6436895	4749	2855	14.10	<0.001	0.4456	11.43					
BH230	Southern Cross Bore	3/7/01	337677	6444621	1605	2206	9.84	<0.001	0.0111	14.62					
BH231	Nillinghoo Bore	3/7/01	354088	6457212	247	1635	6.51	<0.001	0.0749	14.87					
BH232	Quarry Bore	3/7/01	356239	6451427	3406	1501	9.83	<0.001	0.0375	14.99					
BH233	Tyrells Well	3/8/01	345845	6509593	916	391	2.95	<0.001	0.0210	11.55			16.697	15.443	36.375
BH235	Big Six Mile Well Bore	3/8/01	350667	6523989	1797	771	4.17	<0.001	<0.001	13.73					
BH236	Middle Bore	3/8/01	351088	6531142	4056	1465	14.33	<0.001	0.0086	13.97					
BH237	Woolshed Bore	3/9/01	359566	6523732	2981	716	2.35	<0.001	<0.001	16.58					
BH238	Mulga Bore	3/9/01	359552	6540309	11830	3210	12.67	<0.001	<0.001	14.76	0.71598				
BH239	Sandyoota Well	3/9/01	378370	6530880	2690	3774	15.98	<0.001	0.0261	14.02	0.71476		16.728	15.456	36.439
BH240	House Bore	3/9/01	346752	6516302	2256	2106	8.86	<0.001	0.0038	12.71					
BH241	Lucky Hit	3/10/01	408382	6521323	4822	1840	7.32	<0.001	0.8173	11.68			16.589	15.469	36.130
BH242	Salt Well Dam Bore	3/10/01	369366	6510410	10325	2721	13.08	<0.001	0.0707	14.54					
BH244	House Bore	3/11/01	362653	6497169	5409	1307	5.63	<0.001	0.0177	14.40					
BH246	Kemps Bore	3/12/01	342053	6523983	1280	835	5.67	<0.001	0.0374	11.45	0.71381				
BH247	South Martins Bore	3/12/01	332455	6519533	323	102	2.14	0.0032	0.0667	10.95			16.880	15.471	36.821
BH248	Black Hill Wells Bore	3/12/01	327896	6522762	710	317	4.15	<0.001	0.0204	11.86					
BH249	Martins Well House Bore	3/12/01	320829	6516137	446	204	1.87	<0.001	<0.001	10.18	0.71275				
BH251	Castle Rock Bore	3/12/01	332084	6502125	1185	966	5.52	<0.001	0.1405	23.53					
BH302	One Tree Bore	10/23/01	569034	6428262	1505	497	2.19	<0.001	0.4041	12.32					
BH303	Colestead Bore	10/24/01	559411	6407430	2294	773	3.23	<0.001	0.0436	12.59	0.71953				
BH305	Angle Bore	10/24/01	564020	6410226	1517	585	2.18	<0.001	0.0654	12.76					
BH306	Old Kanbara Homestead Bore	10/24/01	558125	6424202	2939	964	4.44	<0.001	0.2161	13.17					
BH307	Elizabeth Bore	10/25/01	511025	6435376	87	159	0.17	<0.001	0.0054	7.28			16.881	15.492	36.660
BH309	Jetpump bore	10/26/01	548850	6451815	2309	1171	4.64	<0.001	0.0430	7.35	0.73403		17.262	15.495	36.498
BH310	LBH0005	10/26/01	548568	6450252	1051	573	1.54	<0.001	0.0679	7.43					
BH311	LA011	10/26/01	542638	6449621	5231	1677	6.95	<0.001	0.0109	14.11					
BH312	Oakdale Explo Bore	10/27/01	517130	6428707	851	614	0.76	<0.001	0.0137	10.60					
BH313	West Mountain Exploration Bore	10/28/01	501446	6421254	634	961	1.94	<0.001	0.0126	2.91	0.72542		16.824	15.494	36.639
BH314	Kadish Bore	10/29/01	494337	6434856	73	58.1	0.06	<0.001	0.0206	8.44					
BH315	Border Bore	10/29/01	549320	6410356	4397	1377	6.25	<0.001	0.0158	12.76					
BH319	Ascot Vale Bore	10/30/01	576448	6412516	1418	500	1.63	<0.001	0.0064	13.19					
BH320	Woolshed Bore	10/30/01	585095	6412239	1289	455	1.42	<0.001	0.0061	13.01					
BH321	Goodenough Bore	10/30/01	589621	6406200	2524	818	3.62	<0.001	0.0102	13.57	0.71471				
BH322	No. 2 Bore	10/30/01	566167	6431161	2525	860	2.78	<0.001	0.8743	12.97					
BH323	Bamboo Bore	10/31/01	568461	6421034	1734	647	2.23	<0.001	0.0438	12.75					
BH325	Eaglehawk House Bore	10/31/01	565766	6417718	1982	673	2.50	<0.001	0.0091	13.36					
BH326	Annies Bore	10/31/01	582676	6422601	1448	519	1.66	<0.001	0.0097	14.67			17.061	15.554	36.927
BH327	Swamp Bore	11/1/01	571716	6410782	1499	562	1.77	<0.001	0.0275	12.64					

BH328	Maynards Bore	11/1/01	584122	6406949	1714	479	2.00	<0.001	0.0076	13.13					
BH329	No. 2 Bore	11/1/01	564538	6406805	1472	536	2.00	<0.001	0.0160	12.42					
BH330	Block 2 Bore	11/1/01	575907	6422492	1250	481	1.73	<0.001	0.0299	13.88			16.874	15.525	36.780
BH331	Clevedale House Bore	11/2/01	552715	6461898	464	229	0.80	<0.001	0.0108	10.46					
BH332	Yallalee Bore	11/2/01	593402	6419902	1661	591	1.97	<0.001	0.2661	14.07					
BH333	Unnamed	11/2/01	589279	6424138	1390	484	1.80	<0.001	0.2107	13.72					
BH334	No. 4 Bore	11/2/01	578390	6405287	1537	525	1.96	<0.001	0.1281	13.75					
BH336	Agents Well	11/3/01	502792	6437622	334	559	1.13	<0.001	0.1601	8.46					
BH337	House Bore	11/3/01	535909	6469290	1472	806	2.57	<0.001	0.0350	10.02					
BH402	New Flow Bore/Lake Ellis Bore	2/8/02	528091	6630716	644	1.10	1.18	<0.001	0.0031		0.71033				
BH422	BHP Bore	2/12/02	528870	6589852	4381	1085	4.01	<0.001	0.0499		0.71958				
BH430	New Bore	2/13/02	505980	6607679	3014	<0.05	1.15	<0.001	0.0132		0.71541				
BH431	Mollies Bore	2/14/02	508018	6629613	2299	14.3	1.22	<0.001	0.0019		0.70797				
BH441	House Bore	2/16/02	567011	6583168	860	483	1.44	<0.001	0.0501		0.71353				
SCK01	No 1 Bore	3/15/01	573174	6437719	1942	660		<0.001	0.0180	12.40					
SCK02	No 3 Bore	3/15/01	574974	6432822	1525	546		<0.001	0.0200	12.90					
SCK03	Farmcote Well	3/15/01	560413	6458095	4369	1698		<0.001	0.0290	12.50					
SCK04	Rangers Bore	3/15/01	556855	6457698	2404	999		<0.001	0.0720	8.30					
SCK05	Old Railway Bore	3/16/01	547780	6482928	1410	868		<0.001	0.0810	8.40					
SCK07	Springs Shear	3/16/01	558246	6475206	472	202		<0.001	0.0270	10.30	0.73374		17.212	15.500	36.894
SCK10	Ironblow Bore	3/16/01	559894	6473624	1066	747		<0.001	0.1300	10.00					
SCK11	Mulga Springs	3/16/01	564596	6474097	2462	769		<0.001	0.0070	13.60			17.415	15.574	37.081
SCK12	Fords Well	3/17/01	547683	6477860	921	304		<0.001	0.0060	11.00			17.638	15.664	37.311
SCK13	Stephens Creek Bore	3/17/01	550385	6475517	277	100		<0.001	0.0180	12.40			17.408	15.538	37.023
SCK14	Hidden Bore	3/17/01	534487	6481988	4784	2389		<0.001	0.0200	6.40			16.621	15.453	36.159
SCK16	Parnell Bore	3/17/01	538545	6478007	4248	2647		<0.001	0.1200	7.20	0.73709		16.213	15.406	35.898
SCK17	Forking Bore	3/18/01	558407	6460426	2628	1829		<0.001	0.0330	8.00					
SCK18	Block 1 Bore	3/18/01	576053	6427041	1347	502		<0.001	0.2000	12.60	0.71942		16.620	15.408	36.347
SCK19	Lizzies Bore	3/18/01	587848	6427694	1369	481		<0.001	0.0100	13.90					
Minimun					73	<0.05	0.06	<0.001	<0.001	2.29	0.70797	0.71518	16.213	15.406	35.898
Median					1885	868	3.62	0.0021	0.0278	12.71	0.71949	0.72223	17.212	15.538	36.927
Maximum					12800	4150	22.05	0.0131	2.8385	23.53	0.73709	0.73170	18.576	15.840	38.397

[a] By MC-ICP-MS.
[b] By TIMS.

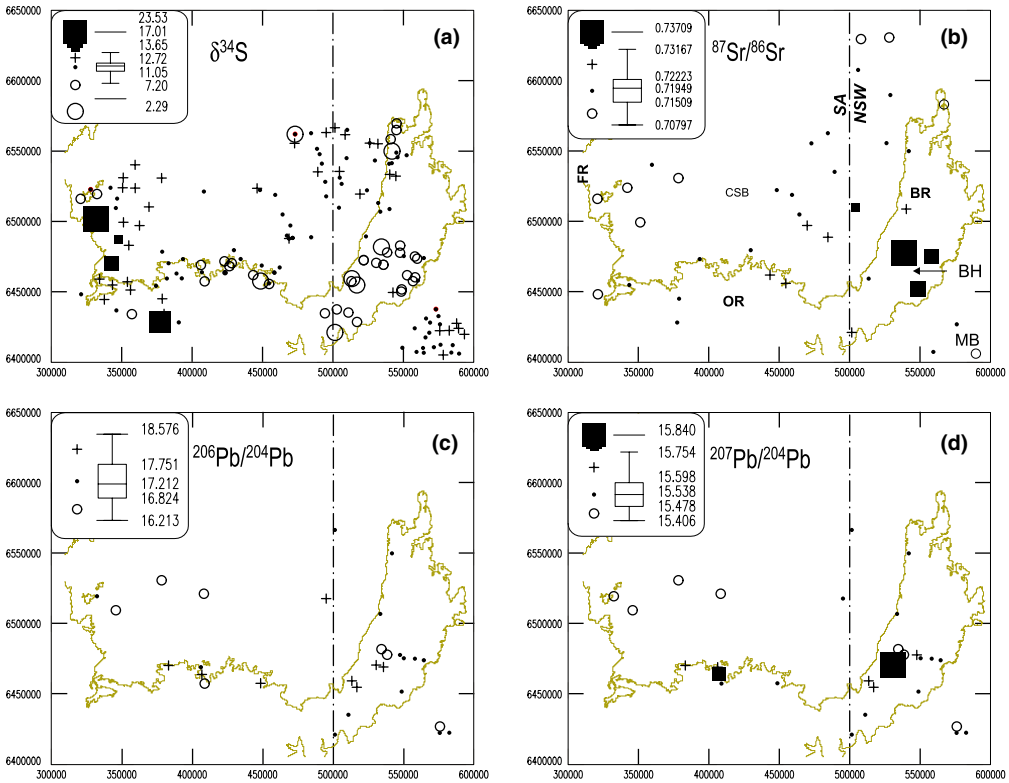

Fig. 3. Geochemical maps of (a) $\delta^{34}S$ (‰ V-CDT), (b) $^{87}Sr/^{86}Sr$, (c) $^{206}Pb/^{204}Pb$ and (d) $^{207}Pb/^{204}Pb$ distributions in groundwaters from the Broken Hill region. The data values are classed according to the boxplot distributions using Exploratory Data Analysis conventions (large circles: lower outliers; small circles: <25th percentile; dot: 25–75th percentile; plus sign: >75th percentile; growing squares: upper outliers; e.g., Tukey, 1977; Velleman and Hoaglin, 1981). See Fig. 2 for abbreviations and map conventions.

$r^2 = 0.49$ (Fig. 4(a)). In general, recharge waters have slightly higher SO_4^{2-}/Cl^- (mass) ratios (0.2–2) than basin waters (0.001–1.4) (Fig. 4(b)), similar to, or higher than, the ratio in local rain water (0.27–2.7) (Blackburn and McLeod, 1983; Bill Ullman, pers. comm.; the authors' unpublished data). The average SO_4^{2-}/Cl^- ratio of the samples (0.51) is significantly higher than that of seawater (0.14). (All seawater data used herein are from Drever, 1997.) The fact that ratios in rainwater are greater than in seawater indicates that an addition of S occurred during atmospheric transport and/or precipitation. The similarity between the SO_4^{2-}/Cl^- ratios of the rainwater and the majority of groundwaters suggests that further increases in both SO_4^{2-} and Cl^- concentrations took place mainly by evaporation, an hypothesis borne out by stable isotope analysis (the authors' unpublished data). However, several samples, particularly – but not exclusively – from the recharge areas, have ratios significantly greater than average rainwater, indicating a further, post-precipitation addition of S (Fig. 4(b)).

There is no clear relationship between groundwater $\delta^{34}S$ values and groundwater salinity or Cl^- concentration (Fig. 4(c)). The recharge waters generally have a lower S isotope composition than the basin waters, suggesting that they contain a ^{34}S-depleted S component.

Fig. 4(d) shows a distribution typical for the mixing of two isotopically different sources: one homogeneous (between +12.5‰ and +14.5‰) and constant, and the other inhomogeneous and variable (see Fig. 11-4 in Krouse, 1980; Kirste et al., 2003). Wakshal and Nielsen (1982) and Chivas et al. (1991) recognised two sources for S in rainfall and gypsum in playa lakes: (1) sea-salt and (2) oxidized volatile biogenic compounds, both of fixed isotopic composition (+20 to +21 and ~0‰, respectively). However, in both studies variations in $\delta^{34}S$ values related more to geographic location than to mixing, suggesting that the variability observed in Fig. 4(d) may reflect mixing between input from atmospheric deposition and bedrock sources. Generally, the basin waters trend toward higher $\delta^{34}S$ values with increasing SO_4^{2-} concentration and the recharge waters toward lower $\delta^{34}S$ values. This isotopic and compositional distinction between the two types of water has been recognised before (Caritat et al., 2001, 2002) and results from a generally poor hydraulic connectivity between the upland regions and the surrounding basins. It has been noted by the same authors that evaporation is a

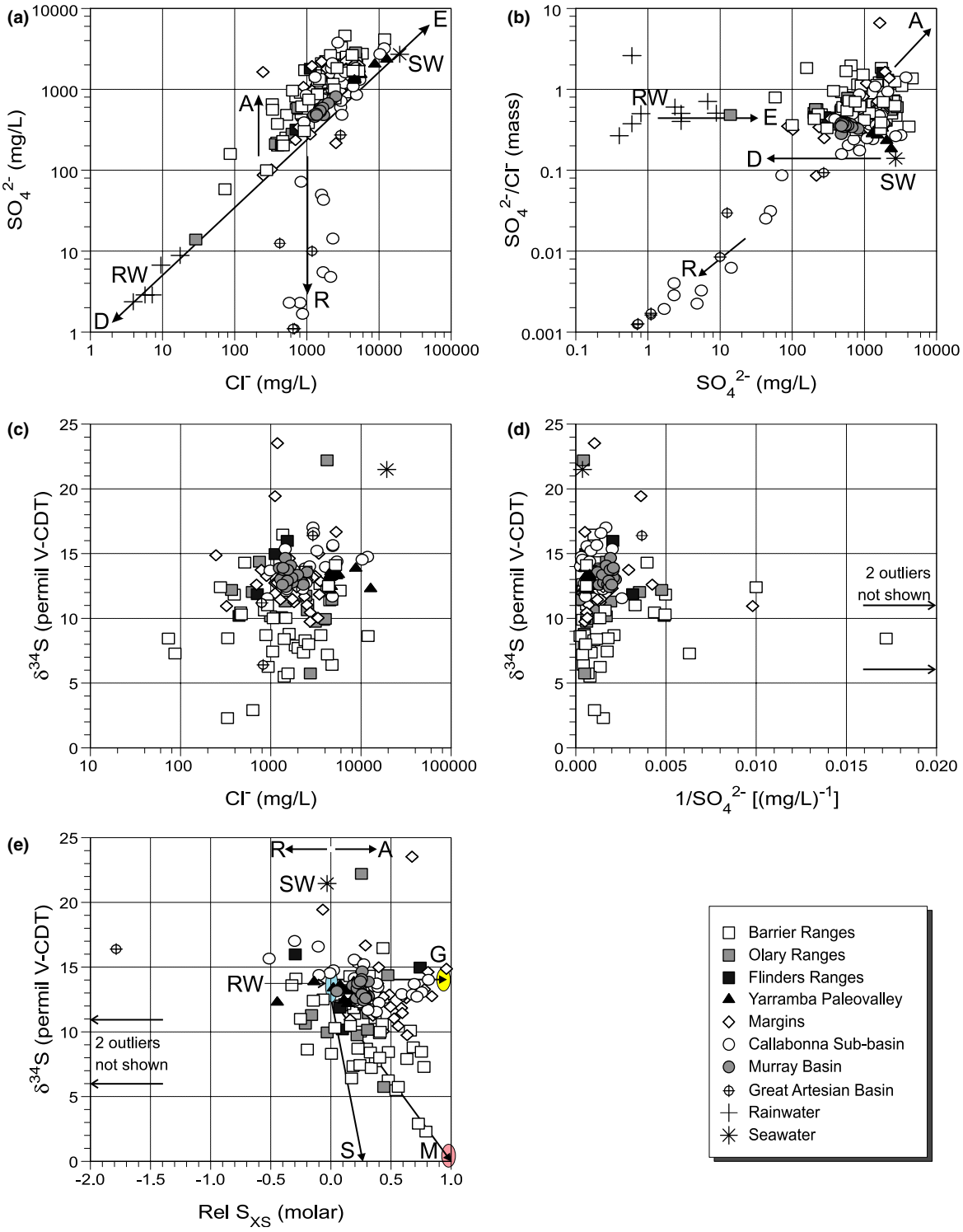

Fig. 4. Diagrams of (a) SO_4^{2-} vs Cl^-, (b) SO_4^{2-}/Cl^- vs SO_4^{2-}, (c) $\delta^{34}S$ vs Cl^-, (d) $\delta^{34}S$ vs $1/SO_4^{2-}$ and (e) $\delta^{34}S$ vs Rel S_{XS} (see text) for the groundwaters from the Broken Hill region. Minor ticks on log axes represent 2x, 4x, 6x and 8x the labelled values. Trends are D, dilution (of seawater); E, evaporation (of rainwater); A, addition of SO_4^{2-}; R, removal of SO_4^{2-} (e.g., SO_4^{2-} reduction). End-members are RW, rainwater (data from this study; Blackburn and McLeod, 1983; and Bill Ullman, pers. comm.); SW, seawater (Drever, 1997); G, gypsum; M, Broken Hill type mineralisation; S, sedimentary pyrite. See Fig. 2 for location of samples.

dominant process affecting the chemical composition of the recharge waters, whereas the basin waters appear to be largely connate, sourced by atmospheric precipitation then evaporated as the sediments were deposited in large inland lakes. The variations in salinity of the basin waters reflect differences in the extent of mixing of connate with meteoric water.

The S isotopic composition of groundwater SO_4^{2-} is influenced by the composition of rainfall and the potential contribution from oxidation of sulfide minerals along the flowpath. The $\delta^{34}S$ of SO_4^{2-} in precipitation from the area could not be measured directly because of the low SO_4^{2-} concentrations in collected rain samples. Instead, this value is estimated indirectly from the average $\delta^{34}S$ of surface gypsum in the area, which is +15.36‰ (data collated from Chivas et al., 1991; Shirtliff, 1998; and the authors' unpublished data). Allowing a fractionation factor between gypsum and dissolved SO_4^{2-} of 1.65‰ (Thode and Monster, 1965) yields a groundwater $\delta^{34}S$ value of +13.71‰. This corresponds well with the average $\delta^{34}S$ of the basin groundwaters (+13.46‰) and is assumed to represent the average composition of atmospheric precipitation in the area, to which the authors assign a range of +12.5‰ to +14.5‰.

The $\delta^{34}S$ of Broken Hill type Pb–Zn mineralisation clusters around 0‰ in the Barrier Ranges and around +4‰ to +7‰ in later vein mineralisation of the Olary Domain (Bierlein et al., 1996a). Sedimentary S or S sourced from early diagenetic pyrite typically displays more negative values than the mineralisation. Bierlein et al. (1996a) interpret ^{34}S-depleted $\delta^{34}S$ values in pyrites to be from mixing with sedimentary S and Chivas et al. (1991) report $\delta^{34}S$ values for pyrites in the Cretaceous Bulldog Shale to be very low at approximately −40‰. Thus, there is the potential to detect groundwaters that contain S originating from atmospheric precipitation versus those that have a component of ^{34}S-depleted, sulfide-derived S, as was suggested elsewhere by Gavrishin and Rabinovich (1971) and Waring et al. (1998). Further, combining the $\delta^{34}S$ data with the $\delta^{18}O$ composition of dissolved SO_4^{2-} yields additional information about where sulfide oxidation may have occurred along the groundwater flowpath and about the likely S isotopic composition of the sulfides (Kirste et al., 2003).

Fig. 4(e) shows a plot of $\delta^{34}S$ vs 'Relative S excess' (Rel S_{XS}), where S_{XS} is calculated as follows for the recharge waters, which are strongly influenced by evaporation:

$$[S_{XS}]_{Recharge} = ([SO_4^{2-}] + [S^{2-}])_{GW} - \left\{ ([Cl^-])_{GW} \cdot \left(\frac{[SO_4^{2-}]}{[Cl^-]} \right)_{RW} \right\} \quad (2)$$

and as follows for the basin and basin margin waters, which are strongly influenced by mixing with connate water

$$[S_{XS}]_{Basin} = ([SO_4^{2-}] + [S^{2-}])_{GW} - \left\{ ([Cl^-])_{GW} \cdot \left(\frac{[SO_4^{2-}]}{[Cl^-]} \right)_{RBGW} \right\}, \quad (3)$$

where square brackets denote concentrations in mmol/L and subscripts 'GW', 'RW' and 'RBGW' refer to 'groundwater sample', 'rainwater' and 'reference basin groundwater', respectively. The $[SO_4^{2-}]/[Cl^-]$ ratio of local 'rainwater' was selected at 0.098 (0.27 as a mass ratio), the value from Fowlers Gap in Blackburn and McLeod (1983), a site inside the present study area. The 'reference basin groundwater sample' was selected from the Callabonna Sub-basin sample subset on the basis that it is: (1) unaffected by SO_4^{2-} reduction (i.e., $SO_4^{2-}/Cl^- >$ seawater); and (2) most representative of the connate basin waters (i.e., highest Cl^-/Br^- ratio; see Caritat et al., 2002). The 'RBGW' sample thus selected is BH039 (Watsons Bore), which has a $[SO_4^{2-}]/[Cl^-]$ ratio of 0.1527.

The dimensionless quantity 'Relative S excess' is then defined as:

$$\text{Rel } S_{XS} = \left(\frac{[S_{XS}]}{[SO_4^{2-}]} \right) \quad (4)$$

and is convenient to highlight small absolute S additions, which stand out more when considered in relation to total SO_4^{2-} concentrations. Several groundwater samples, particularly from the ranges, have both anomalous S concentrations (Rel $S_{XS} > 0$) and low $\delta^{34}S$ values (<+12.5‰) (Fig. 4(e)).

Fig. 4(e) reveals that 3 end-members largely account for the groundwater samples that have experienced an addition of S. These end-members are:

(1) Rainwater: Rel $S_{XS} \sim 0$ and $\delta^{34}S \sim +12.5$‰ to +14.5‰ ('RW' on Fig. 4(e)).
(2) Oxidation of Broken Hill type sulfidic mineralisation: Rel $S_{XS} = 1$ and $\delta^{34}S \sim 0$‰ ('M').
(3) Gypsum dissolution: Rel $S_{XS} = 1$ and $\delta^{34}S \sim +12.5$‰ to +14.5‰ ('G').

The majority of the groundwater samples fall within the triangle defined by these 3 end-members. A potential fourth end-member represents the sedimentary/diagenetic pyrite from Mesozoic/Cenozoic sedimentary sequences (Rel $S_{XS} = 1$ and $\delta^{34}S \sim -40$‰, 'S' on Fig. 4(e)). It must be noted that there is a great distance between the southern extent of the Bulldog Shale and the study area (~200 km, Chivas et al., 1991). Further, this end-member would only apply to groundwater samples collected from sedimentary basins, yet it does not appear to influence the basin waters very much. The recharge samples that fall between the 'M' and 'S' trends are at or above gypsum saturation and are thus likely to have precipitated this mineral, thus decreasing

their Rel S_{XS} values and moving to the left on the diagram.

Thus, interpretation of the S systematics suggests that: (1) S concentration has increased in many groundwaters by processes other than evaporation or mixing with connate basinal water; (2) this introduced S is in many cases depleted in ^{34}S and may be derived from mineralisation in the basement. Thus, an isotopic signature of interaction with mineralised basement can be introduced to, and retained by, the groundwater.

4.2. Strontium system

Strontium in groundwater originates from percolating rainwater, which often has a seaspray Sr component (marine accession) and a dust Sr component. This initial Sr concentration and isotopic signature can then be modified by interaction within the soil and aquifer systems, e.g., by precipitation of carbonates or dissolution of various Sr-containing minerals (weathering), cation exchange, etc. The age and initial ^{87}Rb content of minerals undergoing dissolution are important parameters because, over time, ^{87}Rb decays to ^{87}Sr (with a half-life of 4.88×10^9 a). There is no measurable fractionation of Sr isotopes during mineral precipitation and dissolution. Thus, the Sr isotope composition of groundwater enables one to distinguish better between the sources of Sr (and other weathering products), because seawater (and marine carbonates) and radiogenic and/or 'old' minerals have distinct isotopic signatures (e.g., Faure, 1972; McNutt, 2000).

Fig. 5(a) shows that there is a reasonable correlation between Sr and Cl^- concentrations ($r^2 = 0.59$), but Fig. 5(b) shows also that the Sr/Cl^- (mass) ratio of local rainwater (~0.002–0.004) overlaps with that of groundwater (average = 0.002), and that both are significantly higher than in seawater (0.000413). This, the authors interpret, is because rainwater picks up Sr from dust during precipitation events (increasing the Sr/Cl^- ratio from a originally marine value). Then, Sr in the infiltrating rainwater may either be sequestered in any calcite that precipitates in the soil horizons (calcretes are common in the region; Chen et al., 2002) or taken up by ion exchange, consequently lowering the Sr/Cl^- ratio of soil water and shallow groundwater. Subsequently, the Sr/Cl^- ratio of the groundwater may increase again (and even exceed the rainwater value) through water–mineral interaction along the flowpath. The concomitant increases in Sr/Na and Sr/Cl^- ratios beyond the rainwater field (Fig. 5(b)) indicate addition of Sr for many samples (evaporation alone would not produce such a trend).

The Curnamona groundwaters span a wide range in $^{87}Sr/^{86}Sr$ ratios (nearly 0.030) and show no clear correlation with salinity or Cl^- concentration (Fig. 5(c)). They have relatively radiogenic values (up to 0.737) (Figs. 5(c) and (d)), which is unusual for groundwater from sedimentary basins (Harrington and Herczeg, 2003). Many of the groundwater Sr isotope values are significantly higher than the $^{87}Sr/^{86}Sr$ composition of either seawater during or since the Proterozoic (0.702–0.709; Veizer, 1989) or local rainwater (0.713; Ullman and Collerson, 1994; see Fig. 5(e)). This implies that the higher $^{87}Sr/^{86}Sr$ ratios observed in these groundwaters can not be explained by inheritance from seawater, marine carbonates or rainwater, suggesting an input of radiogenic Sr through water–rock interaction with silicates.

In the Broken Hill region, rocks (granite, gneiss, pegmatite) and minerals (biotite, muscovite, K-feldspar, plagioclase, etc.) belonging to the Paleoproterozoic Willyama Supergroup are highly radiogenic, with $^{87}Sr/^{86}Sr$ compositions commonly $\gg$0.74 (Pidgeon, 1967; Etheridge and Cooper, 1981). In contrast, Adelaidean rocks, which crop out abundantly in the Flinders Ranges to the west of the study area (Fig. 1), have significantly lower mean Sr-isotopic values than Paleoproterozoic craton rocks (Adelaidean shales $^{87}Sr/^{86}Sr$ ratios range from 0.68 to 0.72; Foden et al., 2001). The Sr isotopic composition of the groundwater reflects quite closely this range of source materials (Fig. 3(b)), reflecting basement geology and sediments derived therefrom.

The Sr/Na ratio is useful for distinguishing between Sr released by the dissolution of carbonates or sulfates (enriched in Sr and depleted in Na, yielding higher Sr/Na) versus Sr released by the dissolution of silicates (enriched in Na, yielding lower Sr/Na) (Harrington and Herczeg, 2003). Fig. 5(e) suggests that both carbonates and silicates dissolve to contribute Sr to the groundwater, respectively resulting in high and low Sr/Na ratios. Silicate hydrolysis (low Sr/Na) is a significant process by which Sr of variable, but commonly radiogenic, $^{87}Sr/^{86}Sr$ composition (mostly >0.715) is added to the groundwater. Carbonate weathering yields groundwaters with high Sr/Na, which all have low $^{87}Sr/^{86}Sr$ values (0.712 to 0.715). This carbonate may be hosted within the bedrock and be old, or alternatively may be much younger regolith carbonate (calcrete) in isotopic equilibrium with local rainwater.

The Sr system suggests that (1) the groundwaters have been interacting with minerals originating from the basement rocks (either in the fractured basement itself, or as part of the clastic basin-fill sequence), and that (2) the groundwaters are potentially relatively old since they have had time to weather relatively resistant minerals such as silicates (a suggestion supported by the authors Cl^--isotope data, unpublished).

4.3. Lead system

The Pb isotope composition of groundwater has the potential to directly reflect mineralisation because low-temperature organic or inorganic processes do not fractionate Pb isotopes (Gulson and Mizon, 1979; Gulson,

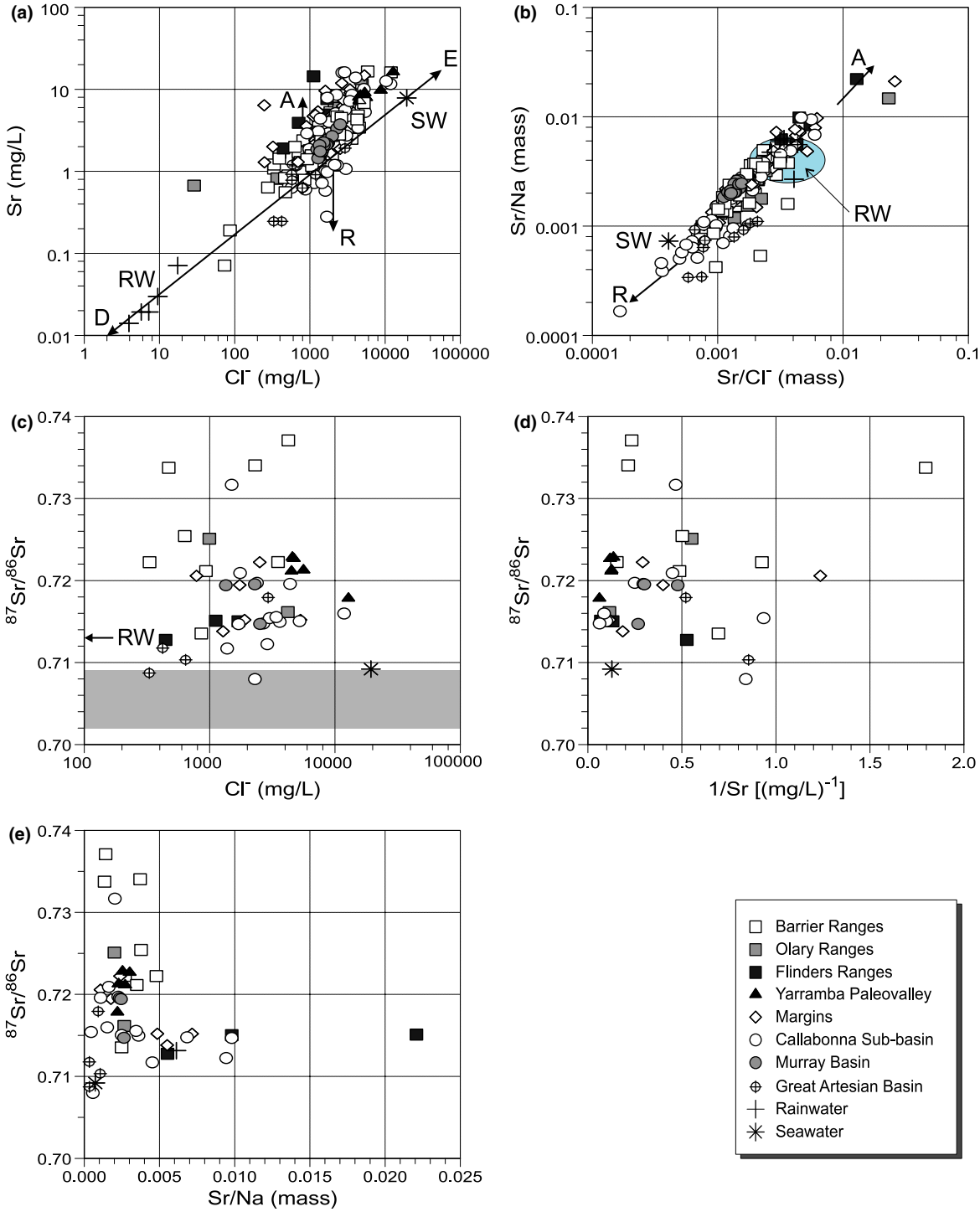

Fig. 5. Diagrams of (a) Sr vs Cl^-, (b) Sr/Na vs Sr/Cl^-, (c) $^{87}Sr/^{86}Sr$ vs Cl^-, (d) $^{87}Sr/^{86}Sr$ vs 1/Sr and (e) $^{87}Sr/^{86}Sr$ vs Sr/Na for the groundwaters from the Broken Hill region. Minor ticks on log axes represent 2x, 4x, 6x and 8x the labelled values. Trends are D: dilution (of seawater); E, evaporation (of rainwater); A, addition of Sr; R, removal of Sr (or addition of NaCl). End-members are RW, rainwater (data from this study; Blackburn and McLeod, 1983; and Bill Ullman, pers. comm.); SW, seawater (Drever, 1997); grey box in (c) represents the range of $^{87}Sr/^{86}Sr$ values during and since the Proterozoic (Veizer, 1989). See Fig. 2 for location of samples.

1986). Various mineralisation types have distinct Pb isotope signatures (Gulson et al., 1985; Gulson, 1986), allowing discrimination between various mineralisation types, or even between barren and economic sulfide accumulations. However, dissolved Pb is prone to adsorb onto solid surfaces along the flowpath, commonly resulting in very low Pb concentrations (<1 μg/L) in groundwater, necessitating the use of ion exchange columns in the procedure.

The relationship between $^{206}Pb/^{204}Pb$ ratios and Cl^- (Fig. 6(a)) suggests a broad tendency for lower Pb isotope ratios with higher Cl^- concentrations or salinity. The relationship between Pb isotope ratios and Zn, a metal common to many Pb-sulfides that is significantly more soluble and mobile in groundwater systems than Pb, is shown on Fig. 6(b) with Zn normalised to Cl^- to remove evaporative/salinity effects. The bulk of the data (see exceptions below) shows a broad tendency for lower $^{206}Pb/^{204}Pb$ ratios to occur with higher Zn/Cl^- ratios (despite the fact that Cl^- itself is also higher, see above). This suggests that samples with a Pb isotope signature more similar to that of the Broken Hill main lode ($^{206}Pb/^{204}Pb$ ratio ~16, Cooper et al., 1969; Gulson et al., 1985; Carr and Sun, 1996) also have more Zn in solution, even when normalised to Cl^-. This is consistent with Broken Hill being a Zn-rich deposit (commonly 10–20% Zn; Stevens and Burton, 1998), and suggests that the Zn/Cl^- ratio may be a useful exploration vector for Broken Hill type mineralisation in the region.

A group of 5 samples (circled in Fig. 6(b)) plot towards the top right hand side corner of the scatter diagram. Of these samples, one is from the Thackaringa Hills (BH152); mineralisation from this area, Thackaringa-style mineralisation, has been documented to have a relatively high $^{206}Pb/^{204}Pb$ ratio (~17–18; Parr et al., 2003), almost coinciding with the value for the groundwater (18.6). Another two samples from that group (BH153 and BH158) are from the same geographic area, whereas the two others are from areas of basin cover further to the NW (BH030) and west (BH212).

It is also clear from the geochemical map (Fig. 3(c)) that all the occurrences bar one (BH030) with high, Thackaringa type, $^{206}Pb/^{204}Pb$ ratios are located in an east-west strip along the southern edge of the Callabonna Sub-basin, i.e., extending directly west from the Thackaringa mineralisation. The geological controls on this pattern are not immediately obvious, as the main grain in the region is striking SW to NE.

Comparing the Pb isotope results with the Rel S_{XS} parameter (Fig. 6(c)) shows that both the group of samples with high $^{206}Pb/^{204}Pb$ ratios mentioned before (Thackaringa type), and a large proportion of the samples with low $^{206}Pb/^{204}Pb$ ratios (more Broken Hill type) have positive Rel S_{XS} values. This could indicate that oxidation of sulfide mineralisation of a certain Pb isotope character was taking place at some point along the groundwater flowpath.

The $^{208}Pb/^{204}Pb$ versus $^{206}Pb/^{204}Pb$ diagram (Fig. 6(d)) has a steep slope (0.82) and the $^{206}Pb/^{204}Pb$ ratios are not abnormally elevated. This indicates that the Pb isotope systematics are not adversely affected by any U mineralisation (Gulson, 1986), which is known to be present in the region, both in areas of outcrop (e.g., Olary Ranges, Mt Painter region) and within the sedimentary cover (e.g., Honeymoon deposit in the Yarramba paleovalley, Beverly deposit NW of Lake Frome).

In terms of $^{207}Pb/^{204}Pb$ versus $^{206}Pb/^{204}Pb$ (Fig. 6(e)), the Pb isotope results plot close to the growth curve that extends from the Broken Hill ore signature to the average background Pb isotope signature. Those samples with the lower $^{206}Pb/^{204}Pb$ ratios (~16.5) may represent a Broken Hill type signature slightly 'diluted' by a minor amount of Pb with higher $^{207}Pb/^{204}Pb$ and $^{206}Pb/^{204}Pb$ ratios (background Pb or other mineralisation type). Six samples have $^{206}Pb/^{204}Pb$ ratios <16.8, which is the upper limit for the 'Broken Hill type', 'late galena' and 'stratabound Pb–Zn deposits' groups of Parr et al. (2003). Of these, two are mineral exploration drillholes: one (SCK16) is from the vicinity of known mineralisation (Parnell Pb–Zn mine, a Broken Hill type deposit; Parr et al., 2003; Barney Stevens, pers. comm.) in the southern Barrier Ranges, the other (BH241) is in the middle of the Callabonna Sub-basin and is a BHP exploration drillhole. None of the 4 other samples (SCK14, SCK18, BH233, BH239) are from near known mineralisation or from exploration drillholes, and thus indicate areas for future exploration. All of the 6 samples may represent either unmixed (proximal) Pb–Zn mineralisation of one of the above types (see Fig. 6(e)), or a mixture of one of these types with another mineralisation Pb isotope signature with higher ratios (e.g., Thackaringa type) or with background Pb.

The samples with higher $^{207}Pb/^{204}Pb$ and $^{206}Pb/^{204}Pb$ ratios may represent various other local ore types recognised in the Broken Hill district (Thackaringa, Pyrite Hill, Ettlewood, etc.; Gulson et al., 1985; Bierlein et al., 1996b; Parr et al., 2003), as discussed above. Alternatively, they can be interpreted as mixtures between various Pb sources, including mixtures of Broken Hill type Pb signatures with background Pb signatures. At this stage, it is difficult to differentiate between these two alternative interpretations.

4.4. Combined sulfur, strontium and lead systems

The relationship between $\delta^{34}S$ and $^{87}Sr/^{86}Sr$ values (Fig. 7(a)) shows that the samples with a sulfide mineralisation signature, i.e., with low $\delta^{34}S$ (<+12.5‰), have a wide range of Sr isotope signatures (0.712–0.737). Of the recharge waters, it is clear that those from the

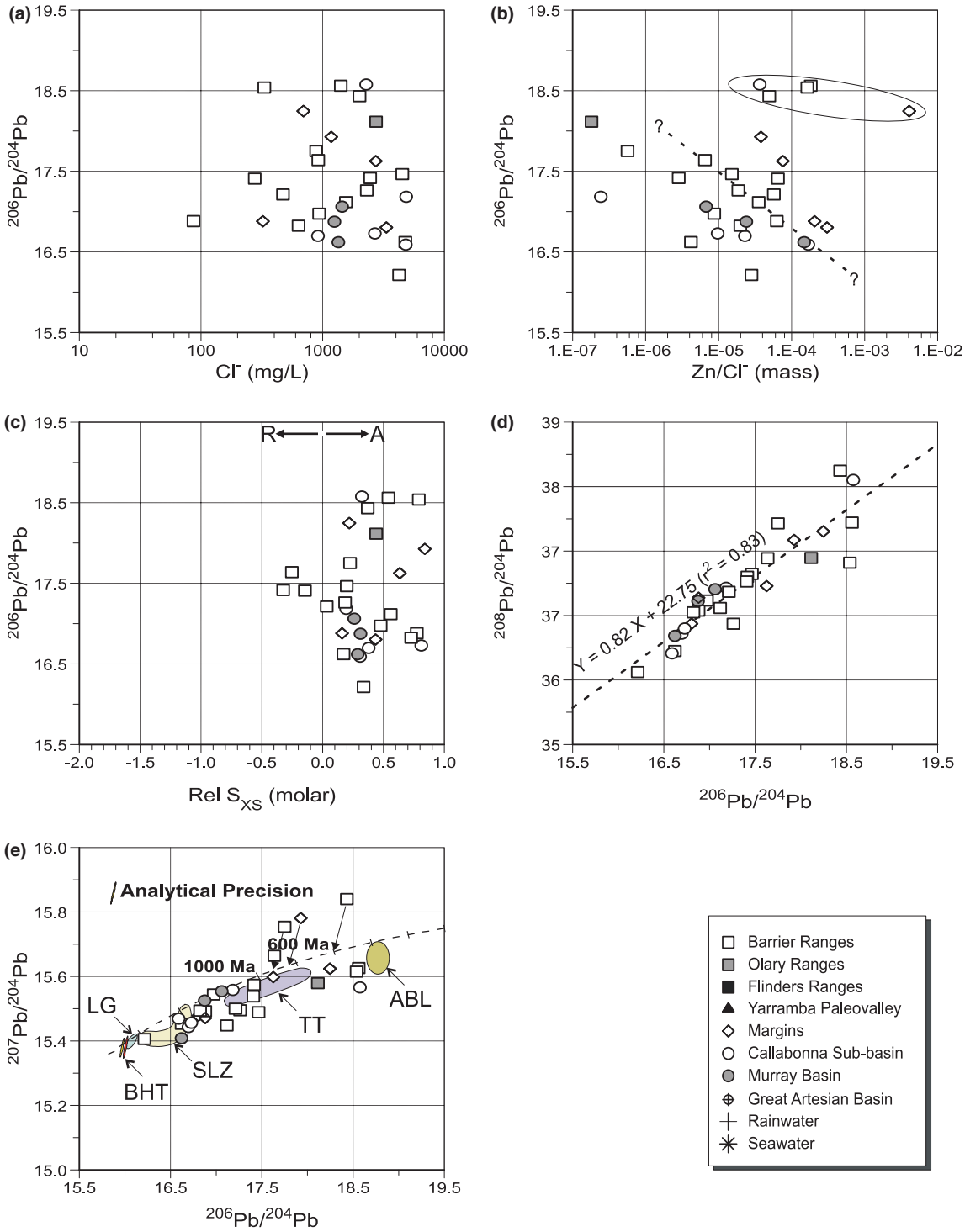

Fig. 6. Diagrams of (a) $^{206}Pb/^{204}Pb$ vs Cl^-, (b) $^{206}Pb/^{204}Pb$ vs Zn/Cl^-, (c) $^{206}Pb/^{204}Pb$ vs Rel S_{XS} (see text), (d) $^{208}Pb/^{204}Pb$ vs $^{206}Pb/^{204}Pb$ and (e) $^{207}Pb/^{204}Pb$ vs $^{206}Pb/^{204}Pb$ for the groundwaters from the Broken Hill region. Minor ticks on log axes represent 2x, 4x, 6x and 8x the labelled values. Trends in (c) are A: addition of SO_4^{2-}; R, removal of SO_4^{2-}. Fields in (e) are BHT, Broken Hill type deposits (two ellipses shown); LG, late galena; SLZ, stratabound lead zinc; TT, Thackaringa type deposits; ABL, average background Pb. These fields and the Mount Isa growth curve are from Parr et al. (2003). See Fig. 2 for location of samples.

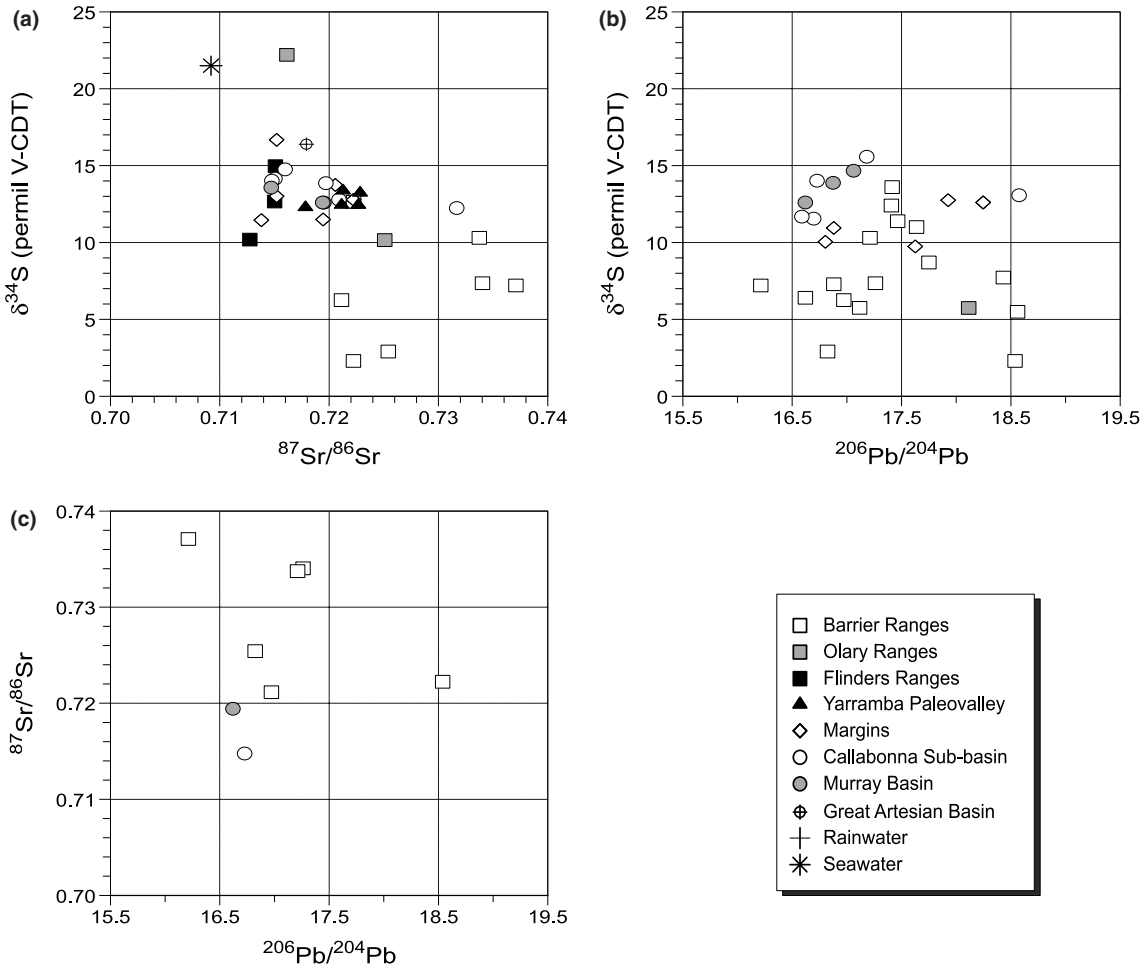

Fig. 7. Diagrams of (a) $\delta^{34}S$ vs $^{87}Sr/^{86}Sr$, (b) $\delta^{34}S$ vs $^{206}Pb/^{204}Pb$ and (c) $^{87}Sr/^{86}Sr$ vs $^{206}Pb/^{204}Pb$ for the groundwaters from the Broken Hill region. See Fig. 2 for location of samples.

Barrier Ranges have both the lowest $\delta^{34}S$ values (Broken Hill type sulfides) and the more radiogenic Sr isotope ratio (Willyama bedrock). The 3 recharge waters with $\delta^{34}S$ of $\sim +10‰$, neatly reflect the bedrock type from which they originate: the one from the Flinders Ranges region has the lowest $^{87}Sr/^{86}Sr$ value (0.714), the one from the Olary Ranges an intermediate value (0.725) and the one from the Barrier Ranges the most radiogenic Sr isotope composition (0.734). A few samples from basins, margins and the Yarramba paleovalley have S isotope signatures that indicate some component of ^{34}S depleted sulfur ($\delta^{34}S < +12.5‰$). Their $^{87}Sr/^{86}Sr$ values mostly low to intermediate (0.713–0.724), except for one Callabonna Sub-basin sample (0.732). All, except one paleovalley sample, have a positive Rel S_{XS}, indicating that low $\delta^{34}S$ sulfur was added, potentially from interaction with mineralisation. The samples with high $\delta^{34}S$ values (>+12.5‰) all have non-radiogenic Sr isotope ratios (0.714–0.718), indicating that they encountered neither sulfide mineralisation nor typical Willyama type bedrock.

Fig. 7(b) shows that the samples with a low $\delta^{34}S$ (<+12.5‰) can have a wide range of $^{206}Pb/^{204}Pb$ values (~16.2–18.6). All the samples with $\delta^{34}S < +10‰$ on Fig. 7(b) have Rel $S_{XS} \geqslant 0$, suggesting possible interaction with a range of different sulfide mineralisation styles as suggested by the Pb isotopic variability. Of all the samples with $\delta^{34}S > +10‰$ on Fig. 7(b), all the basin and margin samples have Rel $S_{XS} \geqslant 0$, whilst the recharge samples have Rel S_{XS} either very close to zero or negative (see Fig. 6(c)). Thus, those basin and margin samples have experienced S addition, but the amount of S added was probably too small compared to the existing pool of S already present in the groundwater to markedly bring down the $\delta^{34}S$ value. The Pb isotope ratios, though, are compatible with Broken Hill type mineralisation being encountered. Again, this indicates that samples *BH241*, SCK18, *BH233*, BH239, *BH206*, BH330,

BH326, BH117, *BH247*, *BH204*, BH205, BH212, BH030 (in order of increasing $^{206}Pb/^{204}Pb$ ratios, *italics*: $\delta^{34}S < +12.5‰$) are from areas worthy of further exploration activity. Of these, only BH241 is an exploration drillhole targeting mineralisation; it supports the interpretation that it is from this bore that the authors get the most 'interesting' basin sample in terms of S and Pb isotopes.

The two basin samples on Fig. 7(c) have Broken Hill type Pb isotope composition and also positive Rel S_{XS} values (not shown). The lack of strong relationships on Fig. 7(c) suggests that the full spectrum of Pb isotope signatures is found across the range of bedrock types encountered in the region, from less to more radiogenic. This implies that areas underlain by less radiogenic Adelaidean bedrock should not necessarily be discounted from the potential to host sulfides with low $^{206}Pb/^{204}Pb$ ratios.

5. Conclusions

This study of S, Sr and Pb isotopes of groundwaters in the Broken Hill region has resulted in a number of significant findings for mineral exploration in the region.

1. The majority of the groundwater samples have undergone a net addition of S and this occurred predominantly, but not exclusively, early in their history (average SO_4^{2-}/Cl^- mass ratio = 0.51 compared to 0.140 for seawater) before significant evaporation or mixing occurred.
2. For a number of samples, that (relative) S excess coincides with low $\delta^{34}S$ values (<+12.5‰), suggesting sulfide mineralisation (~0‰ for Broken Hill type mineralisation) as a possible source for this S; the impact of Mesozoic or younger sedimentary pyrite is minimal.
3. Positive correlation between Sr/Cl^- and Sr/Na ratios, on the one hand, and the high $^{87}Sr/^{86}Sr$ ratios (up to 0.737) of the groundwaters, on the other hand, indicate that Sr with a more radiogenic composition than rainwater (0.713) or Phanerozoic seawater (0.709) has been added to the waters.
4. Sr isotope signatures appear to faithfully reflect the radiogenic character of the basement rocks over (or through) which the drillholes are located. Over Adelaidean basement, the $^{87}Sr/^{86}Sr$ composition of groundwater is clearly lower than over Willyama basement.
5. The groundwaters may have acquired their $^{87}Sr/^{86}Sr$ composition by direct interaction with basement minerals (fractured aquifer systems) or by interaction with clastic material derived from the basement sequences within the basin fill (porous aquifer systems).
6. Sr/Na ratios suggest that silicate hydrolysis is a significant process by which Sr of variable, but commonly radiogenic, $^{87}Sr/^{86}Sr$ composition is added to the groundwater.
7. Pb isotope ratios of the groundwaters suggest that either different mineralisation types are recognisable (e.g., Broken Hill, Thackaringa types), or that mixtures between Broken Hill type mineralisation and other types (or background Pb) are present.
8. Zn, an element commonly associated with Pb mineralisation, shows a moderate increase in concentration (even when normalised to Cl^-) in samples with a more Broken Hill type Pb isotope signature. The groundwater Zn/Cl^- ratio could be a useful vector toward Broken Hill type mineralisation under cover.
9. Groundwater samples collected from the vicinity of Broken Hill type mineralisation (e.g., Parnell mine) or the Thackaringa mineralisation show Pb isotope compositions that indicate a direct genetic link with these types of mineralisation.
10. The Pb isotope systematics are not adversely affected by any U mineralisation in the area, as shown by the steep slope on the $^{208}Pb/^{204}Pb$ versus $^{206}Pb/^{204}Pb$ diagram.
11. Finally, the combination of S, Sr and Pb isotopes with conventional water composition analysis yields strong indicators that, in places, the groundwater has interacted with mineralisation in the subsurface. This powerful tool is shown to work in the vicinity of known mineralisation and thus holds tremendous promise for application to areas of thin to significant regolith cover. Several such new locations worthy of further exploratory efforts are identified herein.

Acknowledgements

This work would not have been possible without the financial support of an Australian Government Cooperative Research Centre (CRC) grant and of the New South Wales Department of Mineral Resources. Neil Lavitt and Rod Dann made significant contributions to parts of this research, for which we are thankful. We gratefully acknowledge the invaluable assistance received from Eleanor Laing-Astolfi and Aleksandra Plasinzka (Bureau of Rural Sciences), Frank Krikowa (University of Canberra), Dave Garnett (Becquerel Laboratories) and Dale Longman, Mike Korsch and Barbara Gardner (CSIRO) in the laboratory, and from Mick Turner, Rod Dann, Leanne Hill, Angela Moonie, Rick Jones, Ian Anderson, Megan Lech, Colleen McMechan, Ian Hutcheon, Jaclyn Brachmanis, Andrew

Retter and Matt Lenahan in the field. We also thank all pastoral leaseholders for granting access to the land and, in the cases of Kalabity, Boolcomatta, Mulyangarie, Corona, Plumbago, Erudina, Pine Point, Fowlers Gap and Paringa stations, for also providing accommodation. Mineral exploration leaseholders are acknowledged for allowing us to carry out this project. The manuscript greatly benefited from the internal reviews by Colin Pain and Jonathan Clarke, and the journal reviews by Angela Giblin and an anonymous referee. PdC publishes with permission from the CEO of Geoscience Australia.

References

Andrew, A.S., Carr, G.R., Giblin, A.M., Whitford, D.J., 1998. Isotope hydrogeochemistry in exploration for buried and blind mineralisation. The State of the Regolith, vol. 20. Geological Society of Australia, Spec. Pub., pp. 222–225.

Bierlein, F.P., Ashley, P.M., Seccombe, P.K., 1996a. Origin of hydrothermal Cu–Zn–Pb mineralisation in the Olary Block, South Australia: evidence from fluid inclusions and sulphur isotopes. Precamb. Res. 79, 281–305.

Bierlein, F.P., Haack, U., Förster, B., Plimer, I.R., 1996b. Lead isotope study on hydrothermal sulphide mineralisation in the Willyama Supergroup, Olary Block, South Australia. Australian Journal of Earth Sciences 43, 177–187.

Blackburn, G., McLeod, S., 1983. Salinity of atmospheric precipitation in the Murray-Darling drainage division, Australia. Aust. J. Soil Res. 21, 411–434.

Callen, R.A., 1990. Curnamona, South Australia. 1:250,000 geological series. Explanatory notes. Sheet SH/54-14. Geol. Surv. South Australia.

Callen, R.A., Sheard, M.J., Benbow, M.C., Belperio, A.P., 1995. Alluvial fans and piedmont slope deposits. In: Drexel, J.F., Preiss, W.V. (Eds.), The Geology of South Australia, vol. 2, The Phanerozoic. Geol. Surv. South Australia Bull., vol. 54, pp. 244–251.

Caritat, P. de, Killick, M.F., Lavitt, N., Tan, K.P., Tonui, E., 2000a. 3D conceptual modelling to aid mineral exploration in the southern Callabonna Sub-basin. MESA J. (Quart. Earth Res. J. Primary Industries and Resources South Australia) 19, 46–47.

Caritat, P. de, Killick, M.F., Lavitt, N., Tonui, E., Dann, R., Turner, M.L., 2000b. Characterisation of the regolith, sediment and groundwater in the Mundi Mundi Curnamona region. In: Broken Hill Exploration Initiative (BHEI): Abst. 2000 Annual Meeting, Broken Hill, May 2000. AGSO Record 2000/10, pp. 16–19.

Caritat, P. de, Kirste, D., Dann, R., Hutcheon, I., 2002. Groundwater composition in the Broken Hill area: salinity and mineral exploration applications. In: Phillips, G.N., Ely, K.S. (Eds.), Proceedings and Field Guide, 'Victoria Undercover' (Benalla, VIC, 30 April–2 May 2002). CSIRO Publishing, Collingwood, pp. 275–278.

Caritat, P. de, Lavitt, N., Kirste, D., 2001. Groundwater geochemistry in the Broken Hill region, Australia. In: Cidu, R. (Ed.), Proc. 10th Intern. Symp. Water–Rock Interaction WRI-10 (Villasimius, Italy, 10–15 June 2001), vol. 1. A.A. Balkema Publishers, Swets, Zeitlinger, Lisse, pp. 489–492.

Carr, G.R., Sun, S.S., 1996. Lead isotope models applied to Broken Hill style terrains – syngenetic vs epigenetic metallogenesis. In: Pongratz, J., Davidson, G.J. (Eds.), New Developments in Broken Hill Type Deposits, 1. CODES Spec. Pub., pp. 77–87.

Chen, X.Y., Lintern, M.J., Roach, I.C. (Eds), 2002. Calcrete: Characteristics, Distribution and Use in Mineral Exploration. Cooperative Research Centre for Landscape Environments and Mineral Exploration.

Chivas, A.R., Andrew, A.S., Lyons, W.B., Bird, M.I., Donnelly, T.H., 1991. Isotopic constraints on the origin of salts in Australian playas. 1. Sulphur. Palaeogeo., Palaeoclim., Palaeoecol. 84, 309–332.

Clarke, W.B., Kugler, G., 1973. Dissolved helium in groundwater: a possible method for uranium and thorium prospecting. Econ. Geol. 68, 243–251.

Cooper, J.A., Reynolds, P.H., Richards, J.R., 1969. Double-spike calibration of the Broken Hill standard lead. Earth Planet. Sci. Lett. 6, 467–478.

Cooper, P.F., Tuckwell, K.D., Gilligan, L.B., Meares, R.M., 1978. Geology of the Torrawingee and Fowlers Gap 1:100,000 sheets 7135, 7235. New South Wales Geological Survey.

Dean, J.R., Bland, C.J., Levinson, A.A., 1982. The measurement of $^{226}Ra/^{223}Ra$ activity ratios in ground water as a uranium exploration technique. J. Geochem. Explor. 19, 187–193.

Drever, J.I., 1997. The Geochemistry of Natural Waters: Surface and Groundwater Environments. Prentice-Hall, Englewood Cliffs, NJ.

Earle, S.A.M., Drever, G.L., 1982. Hydrogeochemical exploration for uranium within the Athabasca Basin, northern Saskatchewan. J. Geochem. Explor. 19, 57–73.

Etheridge, M.A., Cooper, J.A., 1981. Rb/Sr isotopic and geochemical evolution of a recrystallized shear (mylonite) zone at Broken Hill. Contrib. Mineral. Petrol. 78, 74–84.

Faure, G., 1972. Strontium Isotope Geology. Springer-Verlag, Berlin.

Foden, J., Barovich, K., Jane, M., O'Halloran, G., 2001. Sr-isotopic evidence for Late Neoproterozoic rifting in the Adelaide Geosyncline at 586 Ma: implications for a Cu ore forming fluid flux. Precamb. Res. 106, 291–308.

Gavrishin, A.I., Rabinovich, A.L., 1971. Sulfur isotopic composition of sulfate in natural waters from sulfide deposits in the Middle Urals. Geochem. Internat. 8, 550–552.

Giblin, A., Mazzucchelli, R., 1997. Groundwater geochemistry in exploration; an investigation in the Black Flag District, Western Australia. Aust. J. Earth Sci. 44, 433–443.

Gibson, D., 2000. Regolith, landform history and sampling strategies in the Wonnaminta area, Koonenberry Belt. In: Broken Hill Exploration Initiative (BHEI): Abst. 2000 Annual Meeting, Broken Hill, May 2000. AGSO Record 2000/10, pp. 41–44.

Gulson, B.L., 1986. Lead isotopes in mineral exploration. Developments in Economic Geology, 23. Elsevier, Amsterdam.

Gulson, B.L., Mizon, K.J., 1979. Lead isotopes as a tool for gossan assessment in base metal exploration. J. Geochem. Explor. 11, 299–320.

Gulson, B.L., Porritt, P.M., Mizon, K.J., Barnes, R.G., 1985. Lead isotope signatures of stratiform and strata-bound mineralization in the Broken Hill Block, New South Wales, Australia. Econ. Geol. 80, 488–496.

Harrington, G.A., Herczeg, A.L., 2003. The importance of silicate weathering of a sedimentary aquifer in arid Central Australia indicated by very high $^{87}Sr/^{86}Sr$ ratios. Chem. Geol. 199, 281–292.

Hill, S.M., 2000. The regolith and landscape evolution of the Broken Hill Block, Western New South Wales, Australia. Ph.D. Thesis, Cooperative Research Center for Landscape Evolution and Mineral Exploration (CRC LEME), Australian National Univ..

Hill, S.M., Jones, G.L., Foster, K.A., Willis, S.M., Shirtliff, G., West, D.S., Holzapfel, M., 2000. Mineralisation signatures in the regolith of the Broken Hill region. In: Broken Hill Exploration Initiative (BHEI): Abst. 2000 Annual Meeting, Broken Hill, May 2000. AGSO Record 2000/10, pp. 53–56.

Kirste, D., Caritat, P. de, 2002. Geochemical modelling of processes affecting the chemical composition of groundwaters in the Broken Hill region: effects of regolith properties on mineralised zone chemical signatures. In: 16th Australian Geological Convention, Adelaide, 1–5 July 2002. Geol. Soc. Aust. abst. 67, p. 421.

Kirste, D., Caritat, P. de, Dann, R., 2003. The application of the stable isotopes of sulfur and oxygen in groundwater sulfate to mineral exploration in the Broken Hill region of Australia. J. Geochem. Explor. 78–79, 81–84.

Krouse, H.R., 1980. Sulfur isotopes in our environment. In: Fritz, P., Fontes, J.Ch. (Eds.), Handbook of Environmental Isotope Geochemistry, The Terrestrial Environment, 1. Elsevier, Amsterdam, pp. 435–471.

Leybourne, M.I., Goodfellow, W.D., Boyle, D.R., 1998. Hydrogeochemical, isotopic, and rare earth element evidence for contrasting water–rock interactions at two undisturbed Zn–Pb massive sulphide deposits, Bathurst Mining Camp, N.B., Canada. J. Geochem. Explor. 64, 237–261.

McNutt, R.H., 2000. Strontium isotopes. In: Cook, P.G., Herczec, A.L. (Eds.), Environmental Tracers in Subsurface Hydrology. Kluwer Academic Publishers, Boston (Chapter 8).

Miller, W.R., Wanty, R.B., McHugh, J.B., 1984. Application of mineral-solution equilibria to geochemical exploration for sandstone-hosted uranium deposits in two basins in west central Utah. Econ. Geol. 79, 266–283.

Page, R.W., Laing, W.P., 1992. Felsic metavolcanic rocks related to the Broken Hill Pb–Zn–Ag orebody, Australia: geology, depositional age, and timing of high-grade metamorphism. Econ. Geol. 87, 2138–2168.

Parr, J.M., Stevens, B.P.J., Carr, G.R., 2003. Timing of multiple hydrothermal events in the Broken Hill terrane-Evidence from lead isotopes. In: Peljo, M. (compiler), Broken Hill Exploration Initiative: Abst. July 2003 Conf., Geoscience Australia Record 2003/13, pp. 126–129.

Pauwels, H., Baubron, J.C., Freyssinet, P., Chesneau, M., 1999. Sorption of metallic compounds on activated carbon: application to exploration for concealed deposits in southern Spain. J. Geochem. Explor. 66, 115–133.

Pauwels, H., Tercier-Waeber, M.-L., Arenas, M., Castroviejo, Y., Deschamps, Y., Lassin, A., Graziottin, F., Elorza, F.-J., 2002. Chemical characteristics of groundwater around two massive sulphide deposits in an area of previous mining contamination, Iberian Pyrite Belt, Spain. J. Geochem. Explor. 75, 17–41.

Pidgeon, R.T., 1967. A rubidium–strontium geochronological study of the Willyama Complex, Broken Hill, Australia. J. Petrol. 8, 283–324.

Preiss, W.V., 2000. The Adelaide Geosyncline of South Australia and its significance in Neoproterozoic continental reconstruction. Precamb. Res. 100, 21–63.

Sader, J.A., Leybourne, M.I., McClenaghan, M.B., Hamilton, K., Robertson, K., 2003. Groundwater interaction with kimberlites – A geochemical investigation in northeastern Ontario. Explore (Newslett. Assoc. Explor. Geochemists) 118, 1–4.

Shirtliff, G., 1998. Massive gypsum, ferricretes and regolith landform mapping of western Balaclava, Broken Hill, NSW. Honours Thesis, Cooperative Research Centre for Landscape Evolution and Mineral Exploration (CRC LEME), Univ. Canberra.

Stevens, B.P.J., 1980. A guide to the stratigraphy and mineralization of the Broken Hill Block. New South Wales Geol. Surv. Records 20.

Stevens, B.P.J., 1986. Post depositional history of the Willyama Supergroup in the Broken Hill Block, NSW. Aust. J. Earth Sci. 33, 73–98.

Stevens, B.P.J., Barnes, R.G., Brown, R.E., Stroud, W.J., Willis, I.L., 1988. The Willyama Supergroup in the Broken Hill and Euriowie Blocks, New South Wales. Precamb. Res. 40/41, 297–327.

Stevens, B.P.J., Burton, G.R., 1998. The Early to Late Proterozoic Broken Hill Province, New South Wales. AGSO J. Aust. Geol. Geophys. 17, 75–86.

Stevens, B.P.J., Corbett, G.J., 1993. The Redan Geophysical Zone, part of the Willyama Supergroup? Broken Hill, Australia. Aust. J. Earth Sci. 40, 319–338.

Taufen, P.M., 1997. Ground waters and surface waters in exploration geochemical surveys. Exploration Geochemistry. In: Gubins, A.G. (Ed), Proceedings of Exploration 97: 4th Decennial Internat. Conf. Mineral Exploration, pp. 271–284.

Thode, H.G., Monster, J., 1965. Sulphur-isotope geochemistry of petroleum, evaporites and ancient seas. Am. Assoc. Petrol. Geol. Mem. 4, 367–377.

Tonui, E., Caritat, P. de, Leyh, W., 2003. Geochemical signatures of mineralization in weathered sediments and bedrock, Thunderdome prospect, Broken Hill, western New South Wales, Australia: Implications for mineral exploration under cover. Geochem. Explor. Environ. Anal. 3, 263–280.

Tukey, J.W., 1977. Exploratory Data Analysis. Addison-Wesley, Reading, UK.

Ueda, A., Krouse, H.R., 1986. Direct conversion of sulphide and sulphate minerals into SO_2 for isotope analyses. Geochem. J. 20, 209–212.

Ullman, W.J., Collerson, K.D., 1994. The Sr-isotope record of late Quaternary hydrologic changes around Lake Frome, South Australia. Aust. J. Earth Sci. 41, 37–45.

Veizer, J., 1989. Strontium isotopes in seawater trough time. Ann. Rev. Earth Planet. Sci. 17, 141–167.

Velleman, P.F., Hoaglin, D.C., 1981. Applications, Basics and Computing of Exploratory Data Analysis. Duxbury Press, Boston, USA.

Wakshal, E., Nielsen, H., 1982. Variations of $\delta^{34}S(SO_4)$, $\delta^{18}O(H_2O)$ and Cl/SO_4 ratio in rainwater over northern Israel, from the Mediterranean Coast to Jordan Rift Valley and Golan Heights. Earth Planet. Sci. Lett. 61, 272–282.

Waring, C.L., Andrew, A.S., Ewers, G.R., 1998. Use of O, C, and S stable isotopes in regional mineral exploration. AGSO J. Aust. Geol. Geophys. 17, 301–313.

Whitford, D.J., Andrew, A.S., Carr, G.R., Giblin, A.M., 1998. Application of isotope studies of Australian groundwaters to mineral exploration: the Abra Prospect, Western Australia. In: Arehart, G.B., Hulston, J.R. (Eds.), Water–Rock Interaction Proceedings of the 9th International Symposium on Water–rock Interaction (Taupo New Zealand, 30 March–3 April 1998). AA Balkema, Rotterdam, pp. 583–586.

Willis, I.L., Brown, R.E., Stroud, W.J., Stevens, B.P.J., 1983. The Early Proterozoic Willyama Supergroup: stratigraphic subdivision and interpretation of high to low-grade metamorphic rocks in the Broken Hill Block, New South Wales. J. Geol. Soc. Aust. 30, 195–224.

Yanagisawa, F., Sakai, H., 1983. Thermal decomposition of barium sulfate–vanadium pentaoxide–silica glass mixtures for preparation of sulfur dioxide in sulfur isotope ratio measurements. Anal. Chem. 55, 985–987.